Visualization of Materials Penetration into Wood and Morpho-anatomical Analysis Using X-rays

Visualization of Materials Penetration into Wood and Morpho-anatomical Analysis Using X-rays

(X 線を用いた木材への物質浸透の可視化と組織学的影響の解明)

2022

The United Graduate School of Agricultural Science,
Gifu University

Science of Biological Resources
(Shizuoka University)

AYUNI NUR APSARI

Visualization of Materials Penetration into Wood and Morpho-anatomical Analysis Using X-rays

(X 線を用いた木材への物質浸透の可視化と組織学的影響の解明)

AYUNI NUR APSARI

TABLE OF CONTENT

Page

LIST OF TABLES

LIST OF FIGURES

CHAPTER 1

GENERAL INTRODUCTION

1.1 Background

Plywood is a wood product that made from wood veneers glued together with their grains in a perpendicular direction. The important thing of the quality and durability of plywood depends on the adhesive used in manufacturing (Asif 2009). Phenol formaldehyde (PF) is one of the most common moisture-durable adhesives used in plywood. Phenol formaldehyde adhesives are usually used in plywood manufacturing for structural applications in exterior conditions (Kurt 2010; Kurt and Cil 2012).

Plywood veneer mostly produced from rotary cutting of blocks on a lathe. In recent years, the plywood industry has used various hardwood (wood from broad-leaved trees) and softwood (wood from conifer trees) species from industrial forests to be wood veneer (sheet) for their plywood. Those are inferior quality wood that has low density, many defects, weak, and often easily to get attack by fungi and termites (Tanaka et al., 2015).

Currently, low-molecule phenol (LMP) is often used to improve wood properties (Wang and Chui, 2012) by enhancing its dimensional stability and biological features. Copper naphthenate has also been used to increase veneer durability, particularly for protection of the veneer surfaces against staining fungi as a wood preservative (Civardi et al., 2016). Appropriate instruments are needed for quality control of the LMP and copper naphthenate treated veneer to determine the distribution of those materials without wasting the tested material.

X-ray microtomography could be a promising method for non-destructive testing to measure and visualize the micro-distribution of LMP and copper naphthenate with high resolution and three-dimensional (3D) images without damaging the wood (Biziks et al.,

2016; Van den Bulcke et al., 2013; Paris et al., 2014), and also can be used to investigate adhesive penetration until microscopic penetration. X-ray microtomography data can not only determine the distribution of the preservative reagent, but can also map the density of the treated wood and changes to the cell wall (Modzel et al., 2011; Furuno et al., 2004). The penetration phenomena are affected by not only the atomic number of the reagent added to the wood, but also by its concentration, which can be visualized clearly using X-ray microtomography (Gilani et al., 2014).

Although X-ray microtomography is powerful for investigating the inner structure of polymer composite materials, the marginal difference in contrast between carbon-based materials such as petroleum-based plastics or organic materials is still an issue. Thus, we designed and proposed X-ray microtomography scanning setting which appropriate to observe material distribution in as many wood species as it can in same high quality X-ray image, and develop method to calculate adhesive penetration on plywood using conventional roentgen X-ray.

1.2 Objectives of the study

This study has two different research which related into one wood product called plywood. Each research has its own main objective related to wood quality determination. It determines thorough visualization which adopt non-destructive technique to do it. It is because efficiency of testing sample persuades plywood industry and wood resources.

First research main objective focused to understand whether the half-width size will be in the fixed size or not concerning increasing glue spreading rate, different wood veneer density, and wood part (heartwood and sapwood part). Most of the adhesive penetration discussion refers to bonding strength despite environmental aspects that can also be part of the discussion, such as thermal conductivity and bound-water diffusion coefficient.

Second research main objective aims to investigated the effect of wood enhancement material, such as low molecule phenol (LMP) and copper naphthenate on the X-ray image quality. It used as media to observed the distribution of those materials in the wood in order to determine the treated-wood quality.

1.3 Structure of the dissertation

This thesis consists of five chapters. Chapter 1 presents general introduction, background, and objectives of the study. It includes explanations about recent issue related to phenol-formaldehyde uses as modification agent and adhesive material, and non-destructive testing using many kinds of X-ray apparatus that widely use nowadays.

Chapter 2 introduced phenol-formaldehyde (PF) resin usage not only as worldwide known wood adhesive, but also as wood extractive to improve physical properties of the treated wood. This chapter also introduced copper (Cu)-based wood preservative that protect wood from decay caused by biological agent and environmental aspect. Based on all reagents used in this PhD research, the distribution phenomena of it should be investigated. Thus, X-ray visualization technique introduced thoroughly in this section.

Chapter 3 discusses relationship between half-width size which define as resin-rich region in the plywood with increasing glue spreading rate, using different wood veneer density, and different wood part (heartwood/sapwood). The non-destructive testing was performed using a classic, conventional, simple roentgen X-ray. The method to calculate half-width which was developed explain thoroughly in this section.

Chapter 4 discusses the investigation of the distribution of low molecule phenol (LMP) and copper naphthenate on the wood veneer using X-ray microtomography in two- and three-dimensional X-ray images. the applicability of X-ray microtomography to distinguish nano-anatomical elements of wood (wood cell wall, lumen, among other variables), and the

reagents (LMP and Cu) on LMP and copper naphthenate treated-wood using seven wood species was tested and explain thoroughly in this section. The X-ray scanning setting and X-ray image field of view to investigate the distribution of LMP and Cu was established in this section too.

Chapter 5 provided the general conclusion of the study.

CHAPTER 2

LITERATURE REVIEW

2.1 Phenol-formaldehyde resin

2.1.1 Phenol-formaldehyde as adhesive

PF adhesives is a poly-disperse systems with intricate formulation reaction schemes, one would not anticipate that long and short polymer chains would be similarly tagged. Phenol formaldehyde (PF) adhesive is both organic and has a density of around 1.5 g/cm^3 after curing. It is made mostly of carbon, hydrogen, and oxygen and has a high carbon content (Paris *et* al., 2014). Regarding moisture resistance, phenol formaldehyde (PF) is regarded as one of the most enduring adhesives (McKinley *et* al., 2016). The capacity of the phenolic groups to infiltrate the wood cell wall has been proposed to prevent water penetration, reduce swelling, and distribute stresses over a larger volume of the bonded assembly (Frihart 2009). For exterior use, phenolic adhesives like phenol formaldehyde (PF) and phenol resorcinol formaldehyde (PRF) are typically utilized in the production of plywood (Kurt, 2010 in Kurt 2012).

PF adhesive penetration into wood usually discussed related to the bonding strength of the plywood. Penetration is affected by the molecular weight distribution, viscosity, solids content, and surface tension of the adhesive's liquid phase. Adhesive penetration caused "adhesion" mechanism, which affects how the boundary layer and substrate interact. Covalent bonds, secondary chemical bonds caused by electrostatic forces, mechanical interlocking, or other processes may represent the mechanism. The idea of mechanical interlocking obviously depends on the adhesive phase penetrating deeper than the exterior wood surface. Additionally, the amount of surface area in contact between the adhesive and the cell wall influences the overall adhesion force brought on by covalent

bonding and subsequent chemical bond formation. More potential for the formation of chemical bonding results from more flow along the lumen surfaces. It's possible that the penetration process changes the cell wall's characteristics. The cell wall may expand or its constituent parts may undergo chemical modification. (Marra, 1992).

The visualization of PF adhesive penetration commonly discussed to clearly show the penetration phenomena. In addition, additives may be added to the PF adhesive to increase X-ray attenuation coefficient. Adding additives may change original characteristics of PF adhesive. Studies have used tools including X-ray fluorescence microscopy (XFM) and nanoindentation to successfully identify adhesive penetration into cell walls (Jakes et al 2015).

2.1.2 Phenol-formaldehyde as wood extractive

Phenol/formaldehyde (PF) resins are well-known as adhesive whereas in the 1940s, Stamm and Seeborg introduced phenol resin impregnated veneers. PF resins can be categorized based on different prepolymer characteristics. In the wood industry, alkaline catalyzed resoles are the most common PF systems. Due to the alkalinity of commonly used resins, after PF resin treatment, wood typically takes on a reddish-brown hue (Furuno et al., 2003). Molecular weight, viscosity, the type of catalyst used (such as NaOH or NH_3), or pH value can all be used to further categorize and distinguish resols. Low molecular weight PF (lmwPF), medium molecular weight PF (mmwPF), and high molecular weight PF are the three categories into which PF resols are divided (hmwPF). Several writers (Furuno et al., 2016; Biziks et al., 2015) have already reported on the good impregnation behavior of lmwPF.

Because the molecular scale of the impregnating chemicals affects their penetration into the wood cell walls, the molecular weight of the resin utilized in PF resin

treatments should be taken into consideration. Low molecular weight PF resin treatment that known as a wood-preservation technique for the prevention of biodeterioration could suppress an attack by decay fungi as well as termites at about 10% to 15% resin loading (Ryu et al. 1991). According to some studies (Furuno and Goto 1978, 1979, Imamura et al. 1983, Kajita and Imamura 1991), resin with a low molecular weight quickly penetrates cell walls and contributes to features like dimensional stability, whereas resin with a greater molecular weight merely fills the cell lumina and so contributes very little to dimensional stability.

In contrast to PF resins, which are made of a water solution of polymer molecules (oligomers) with different molecular weights and shapes, wood is a porous material with two different types of internal voids: big voids like cell lumina and pit apertures, and cell wall microvoids. The large pore system, which includes the lumens of various fiber types, vessels, rays, and libriforms, among others, is first exposed to treatment solutions with oligomers of varying average molecular weights during impregnation using LmwPF. In the cell wall, the oligomers diffuse from the fiber lumen (Li *et* al., 2021) (Figure 2.1). The molecules in the therapy solution that are filling the accessible empty microvoids in the cell wall eventually expand the cell wall, filling them with molecules that are permanent (bulking).

2.2 Copper (Cu)-based wood preservative

Alkaline copper-based quaternary, azoles, and/or borates are well-known and efficient waterborne wood preservative solutions for solid wood. Wood preservatives may be employed to improve the decay and insect resistance of wood product in solid form or composite wood. The benefits of waterborne formulations with micronized copper carbonates and a co-biocide to control copper-tolerant fungus include relative affordability,

minimal copper leaching from treated wood, and less corrosion when in contact with metal fasteners and connectors. When wood is treated with micronized copper (MC), with chemical formula $CuCO_3 \cdot Cu(OH)_2$, Cu reacts with wood in some cases, but some of it also lingers as unreacted Cu particles, creating a reservoir effect. Cu in its soluble state, as Cu^{2+} ions, is primarily responsible for the effectiveness of Cu-based wood preservatives against fungi that damage wood.

Other copper-based wood preservative which widely used after chromated copper arsenate (CCA) cannot be used anymore is copper amine. The fixation mechanism of Cu from Cu-amine preservatives in treated wood is thought to be complexation or ion exchange of Cu complex cations at the sites of proton dissociation from weak acid sites of wood. $[Cu(Mea)_{2\text{-}H}]^+$ formed at pH near nine is an active species, and the less stable protonated part of Mea ligand may be exchanged by positively charged wood acidic groups. Accordingly, stable complexes are formed by interaction of $[Cu(Mea)_{2\text{-}H}]^+$ with carboxylic acid and phenolic hydroxyl groups, with coordination sites of the copper atom being occupied by the deprotonated O atoms at wood acidic groups and the other two sites binding Mea molecules. This coordinate bond seems to occur only at dissociated acid groups, which may be the driving force to attract the cationic $[Cu(Mea)_{2\text{-}H}]^+$ and, therefore, shows a very close relationship with cation exchange capacity (CEC) of wood (Lee and Cooper 2012).

Other copper-based wood preservative is copper naphthenate. By reacting copper with naphthenic acid, a byproduct of oil refining, copper naphthenate is created (Morrell, 2018). A dark-green liquid called copper naphthenate, an organometallic chemical, gives the wood its color. After several months of exposure to weather, the treated wood develops a light brown color due to weathering. If heat is applied while treating the wood, the color of the wood might range from light brown to chocolate brown (Cheremisinoff and Rosenfeld, 2010). Since it is not classified as a pesticide with a restricted usage, copper naphthenate

(CuN) has reemerged as an alternate method. In both above ground and ground contact field experiments as well as laboratory investigations, CuN has demonstrated broad-spectrum efficacy against insects and rot fungus. For ground contact applications, retentions between 0.88 and 1.92 kgm^{-3} (copper as metal), depending on the commodity, are required. The compound is made up of the building blocks R-COO-Cu-OOC-R, where R is any of the saturated C_{10}–C_{40} hydrocarbons that include cyclopentane and/or cyclohexane groups. Neodecanoic acids have been studied as potential replacements for naphthenic acids, and field staking performance has proven encouraging. Effusion of a CuN/boron paste in Douglas fir heartwood has been observed. Water-soluble CuN combined with borates is also utilized for corrective bandaging of poles (Barnes, 2001).

2.3 X-ray visualization technique

2.3.1 X-ray densitometry

In research on tree growth and wood quality, the technique of X-ray densitometry is frequently used to gradually measure density (specific gravity) along a radial strip of wood. Analysis of wood features including ring width, latewood proportion, earlywood and latewood width, and density is possible with radial profiles of density. Principles of densitometric measurements based on X-ray such as radiography is the common X-ray one.

X-ray radiography is the process of taking an image of a projected object using an X-ray beam that is passed through the object. A digital detector or a photographic film are used to capture an image. The attenuation of X-rays, which is proportional to the atomic number and the quantity of atoms in the beam path, determines the gray levels of this X-ray image. The radiography of a wood sample of constant thickness depends mostly on

density difference because the atomic composition of wood is relatively stable, making the instrument for detecting wood density simple to calibrate (Jacquin et al., 2017).

2.3.2 X-ray microtomography

X-ray microtomography is a method for nondestructively characterizing material microstructure in three dimensions with a micron-level spatial resolution (Landis et al, 2010). In addition to mapping the density of the treated wood and changes to the cell wall, X-ray microtomography data can also be used to determine the distribution of the preservative reagent (Modzel et al., 2011; Furuno et al., 2004). Utilizing X-ray microtomography, it is possible to clearly see how the quantity of the reagent applied to the wood affects the penetration phenomena in addition to its atomic number (Gilani et al., 2014).

Although X-ray microtomography is effective for examining the internal structure of polymer composite materials, the slight contrast difference between carbon-based materials, such as biological materials or plastics made from petroleum, is still a problem. As a result, practically all earlier research involved the chemical or adding of contrast media to materials before X-ray microtomography (Paris et al., 2014; Modzel et al., 2011; Furuno et al., 2004). For industrial applications like quality control, the addition or modifications is insufficient.

The morphological evaluation of carbon fiber reinforced polymer (CFRP) materials may now be done thanks to the development of a sub-microscale greater contrast CT equipment that is appropriate for carbon-based materials (Garcea et al., 2018). Oishi and Tanaka (2020) used six X-ray microtomography machines to attempt to directly examine adhesive bondlines of plywood and glulam, and they were successful in visualizing the wood adhesive at the bondlines without the inclusion of any additional materials or chemical

alterations. The field of view (FOV) in this investigation, however, was only at a maximum of 3.6 mm, which is inadequate for industrial applications.

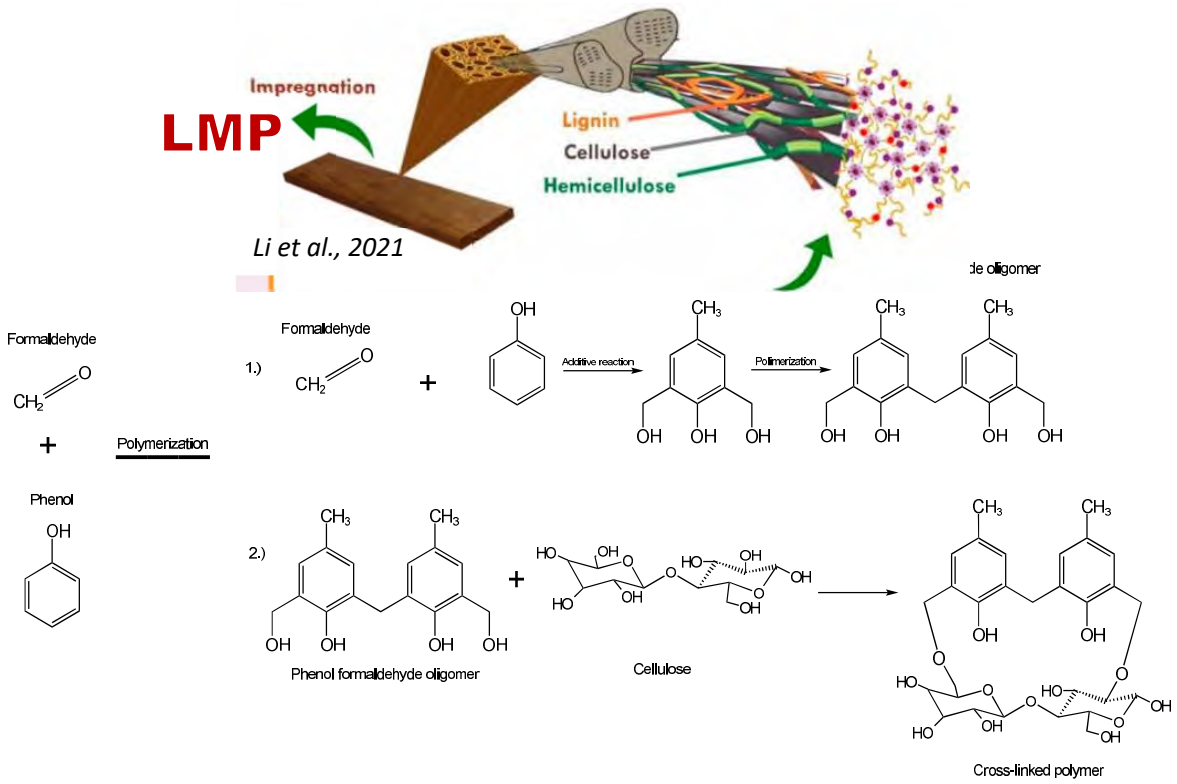

Figure 2. 1 Schematic of the chemical reactions of wood cell wall components with PF Resin

CHAPTER 3

EFFECT OF PHENOL-FORMALDEHYDE ADHESIVE SPREADING RATE AND VENEER DENSITY ON SUGI (*Cryptomeria japonica* (L.f.) D.Don) PLYWOOD

3.1 Introduction

Plywood is a wood product that made from wood veneers glued together with their grains in a perpendicular direction. The important thing of the quality and durability of plywood depends on the adhesive used in manufacturing (Asif 2009). Phenol formaldehyde (PF) is one of the most common moisture-durable adhesives used in plywood. Phenol formaldehyde adhesives are usually used in plywood manufacturing for structural applications in exterior conditions (Kurt 2010; Kurt and Cil 2012). The flow of PF adhesive into the wood cellular structure and infiltration into the cell walls create the wood adhesive interphase (Jakes et al. 2015). The pressure applied on the PF adhesive will affect the adhesive penetration (Cognard 2005).

It is important to investigate the adhesive penetration through the adhesive interphase on plywood. Tanaka (2018) developed a geometrical model of wood cells and adhesive penetration at the veneer-veneer interface of plywood. There are resin-rich region and non-resin region in the geometrical model of 5-ply softwood plywood. The resin-rich region defined as adhesive penetration. Adhesive penetration is categorized into four scales of penetration, namely, macroscopic penetration, microscopic penetration, nanoscale penetration, and angstrom-scale penetration (Laborie 2002). The depth of adhesive penetration is influenced by adhesive parameters (viscosity), substrate parameters (grain angle; earlywood or latewood), and processing parameters (bonding pressure; open time) (White 1975). Optimum adhesive penetration information is important of the efficiency in using the adhesive (Kurt and Cil 2012).

X-rays can be used to investigate adhesive penetration until microscopic penetration. Since the last century, X-ray has been used for wood inspection (Worschitz 1932; Fisher and Tasker 1940; Tomazello et al 2008) consequently, considering the X-ray apparatus as a potential tool for quantitative analysis. Based on research conducted by Tanaka et al. (2012), the X-ray apparatus can be used to quantitatively measure the moisture content distribution in plywood (Tanaka and Shida 2012). However, limitation of knowledge regarding the quantitative analysis of adhesive penetration in plywood requires further research. In a study by Ferrtikasari et al. (2019), it was stated that the qualitative analysis of the X-ray computed tomography image can clearly show the penetration of PF adhesive into lathe check on plywood at a glue spreading rate of 225 g/m^2 and elucidate the relationship between increasing glue spreading rate of plywood and its thermal conductivity (Ferrtikasari et al. 2019). Research conducted by Tanaka et al. (2015) stated that the PF adhesive in wood can be visualized clearly because the mass attenuation coefficient is different between wood and PF. Thus, the PF adhesive visible to visualize in the wood using X-rays (Tanaka et al. 2015).

This study focused to understand PF adhesive penetration size which define as half-width. The effect of increasing glue spreading rate, different wood veneer density, and wood part (heartwood and sapwood part) on the half-width size were investigated. The method to calculate half-width was developed. Other following definition to avoid confusion is term peak-height as PF adhesive concentration.

3.2 Materials and methods

3.2.1 Specimen preparation

Five-ply sugi (*Cryptomeria japonica*) plywood was made from low-, medium-, and high-density heartwood with density values of 0,281 – 0,309 g/cm^3, 0,319 – 0,343 g/cm^3, and 0,346 – 0.372 g/cm^3, respectively. The medium-density sugi sapwood

plywood was made with range of density at 0,320–0,340 g/cm^3. PF adhesive with solid content 48 % was used in this study. Heartwood plywood was made using three glue spreading rates: 75 g, 150 g, and 225 g. Sapwood plywood was made using four glue spreading rates: 75 g, 150 g, 225 g, 300 g. Plywood manufacturing was performed by cold-pressing and hot-pressing at 1 MPa for 20 min **(**Ferrtikasari *et al.* 2019) **(**The properties of the X-ray plywood sample are shown in Table 3.1. Samples for X-ray assessment were cut with dimension 10 mm × 100 mm x plywood thickness for all plywood.

3.2.2 X-ray scanning

An X-ray apparatus, SR-1010 (Softex Co., Ltd., Ebina, Japan) equipped with a digital X-ray sensor (NX-04H, Softex Co., Ltd.), was used. The sample was scanned on a bondline section with 21.5 kV tube voltage, 3 mA tube current, exposure time of 50 s, and a 416-mm-thick polytetrafluoroethylene (PTFE) filter. A schematic of the X-ray photography set-up is shown in Fig. 3.1.

3.2.3 Adhesive penetration analysis based on X-ray images

The X-ray image of the plywood sample was divided into seven lines using ImageJ 1.48v (2014) software to obtain seven plot profiles. The gray value of the poly(methyl methaceylate) (PMMA) block area was used to obtain the equation for the PMMA-equivalent thickness (Fig. 3. 2). This equation was used to convert the gray values of the plot profiles. The converted plot profile was calculated using a certain mechanism to obtain the adhesive penetration and adhesive concentration in plywood.

The effects of the glue spreading rate and veneer density on the half-width were analyzed using two-way analysis of variance (ANOVA).

3.3 Results and discussion

3.3.1 Visualization of PF adhesive penetration on sugi plywood

Adhesive penetration was successfully visualized using an X-ray apparatus. Fig. 3.3a clearly shows the plywood X-ray image. The X-ray setting is one of the determinants in the clear and successful visualization of X-ray images. In this study, the low X-ray tube voltage in the X-ray setting was used to visualize the adhesive penetration in heartwood and sapwood plywood with low, medium, and high veneer densities using various levels of glue spreading rates (75, 150, 225, and 300 g/m^2).

The seven-plot profile from seven representative lines on each X-ray image was obtained using ImageJ 1.48. The peak that represented the glue line was pointed out, and the rest were the latewood peaks (Fig. 3.3a). The adhesive that penetrated the lathe check area was estimated to make the glue line peak broader than the glue line, which has no lathe check penetration (Fig. 3.3b). However, the adhesive inside the lathe check has its own peak, which was not part of the general glue line peak.

3.3.2 PF adhesive penetration on sugi plywood

The seven-plot profile was converted into a PMMA-equivalent thickness value. This was done in order to understand the penetration of the adhesive in the plywood and the concentration of the adhesive in relation to the glue spreading rate. An example of a successful converted plot profile is shown in Fig. 3. 4. After converting the plot profile, the mechanism for calculating the penetration depth of the glue was developed in this study and is shown in Fig. 3. 5.

The base point of the peak should be determined based on the horizontal inequality position of the base point. After the peak height was obtained, the height of the graph was divided by two, which was the way to obtain the middle line of the graph. Then,

the length of the middle line of the graph, which is defined as the half-width occurred. The half-width of the peak was considered as the adhesive penetration depth. The peak height was considered as the adhesive concentration. The half-width and peak-height were obtained from the calculation of the glue line peak (Fig. 3. 6). The half-width (adhesive penetration) value obtained from various glue spreading rate and veneer density was investigated to see the relations between them (Fig. 3. 7).

The half-width was within the range of 0,3 – 0,9 mm and was approximately 0,5 mm on average, regardless of the glue spreading rate or veneer density. This finding is similar to that reported by Modzel *et al.* in 2011 that the penetration depth of the adhesive in the oak, Douglas-fir, and poplar were 400 μm, 100 μm, and 400 μm, respectively (Modzel *et al.* 2011). These results support the idea that glue penetration into the veneer in plywood manufacturing is constant, regardless of the glue spreading rate, veneer density, or the wood species of the veneer. The smallest half-width value (= 0,3 mm) occurred near the boundary between earlywood and latewood (Fig. 3. 8), suggesting that the existence of latewood in the veneer might limit the adhesive penetration. This limitation may lead to the consistency of the average half-width value without regard to the glue spreading rate or veneer density.

The adhesive concentration (peak height) increased along with increasing the glue spreading rate. The peak height of the heartwood plywood with low, medium, and high veneer densities showed the same trend (Fig. 3. 9a, 9b and 9c). The peak height increased with increasing glue spreading rate. In addition, regarding the sapwood-veneer plywood, the maximum peak height was obtained at the maximum spreading rate of 300 g/m^2 (Fig. 3. 9d). These results indicate that the concentration of the adhesive at the bondline is increased by increasing adhesive spreading rate.

The statistical analysis using two-way ANOVA method did not reveal any significant effect of glue spreading rate, veneer density, or their interactions on the half-width value (Table 3. 2).

3.4 Conclusion

We successfully evaluated the concentration profile of sugi plywood with a low X-ray tube voltage. The PF adhesive penetration in the sugi plywood had values of 0,3–0,9 mm, with an average of 0,5 mm. In this experiment, using sugi plywood, it was shown that the existence of latewood might limit the PF adhesive penetration. On the other hand, the PF adhesive concentration in the glue line increases with increasing veneer density and glue spreading rate. Findings from this study would be useful in the analysis of a plywood's quality and durability.

Table 3. 1 The dimensions and densities of the X-ray plywood samples

Veneer type	Veneer's density group	Spreading rate (g/m^2)	Dimension (mm)			Weight (g)	Plywood density (g/cm^3)
			R	T	L		
Heartwood	Low	75	10,03	17,31	100,42	6,11	0,351
	Medium		9,39	17,74	98,28	6,54	0,400
	High		10,22	17,89	100,62	7,75	0,421
	Low	150	9,36	16,59	100,00	5,92	0,381
	Medium		10,39	17,13	100,68	7,92	0,442
	High		10,63	17,41	100,34	7,89	0,425
	Low	225	10,33	15,58	100,33	6,92	0,428
	Medium		10,06	16,59	100,80	7,45	0,443
	High		10,23	16,75	100,73	8,36	0,484
Sapwood	Medium	75	9,33	18,08	100,51	5,77	0,340
		150	10,77	17,66	100,48	6,73	0,352
		225	10,13	17,48	100,47	6,61	0,372
		300	10,25	16,90	100,30	6,52	0,375

Table 3. 2 Results of the two-way ANOVA of veneer density and glue spreading rate in relation with PF adhesive penetration (half-width) on Sugi heartwood plywood

Variation factor	Sum of squares	Degree of freedom	Mean of Squares	F value		F critical (5%)
Veneer Density	0,009294	2	0,004647136	0,511127732	<	3,18
Spreading rate	0,002184	2	0,001091854	0,120090442	<	3,18
Interaction	0,086737	4	0,021684153	2,384989672	<	2,56
Residue	0,463688	51	0,009091927			
Total	0,561903	59				

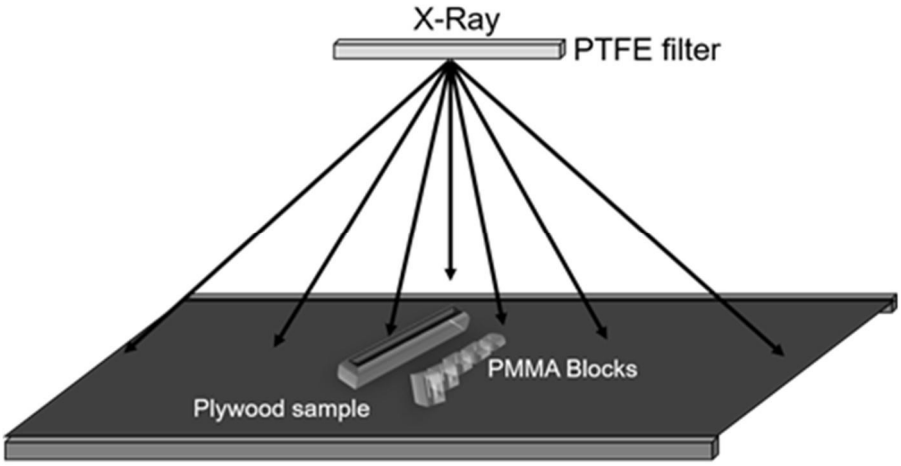

Figure 3. 1 Schematic of the X-ray photography condition.

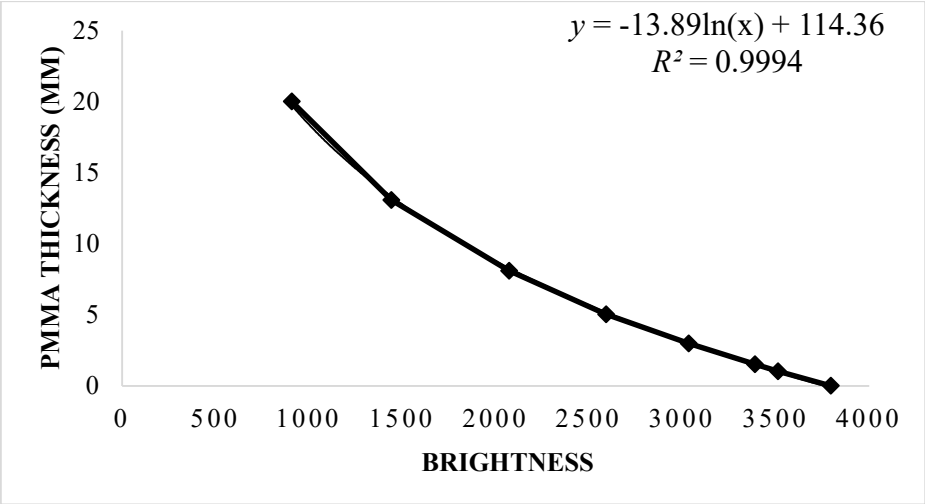

Figure 3. 2 Equation of the PMMA-equivalent thickness

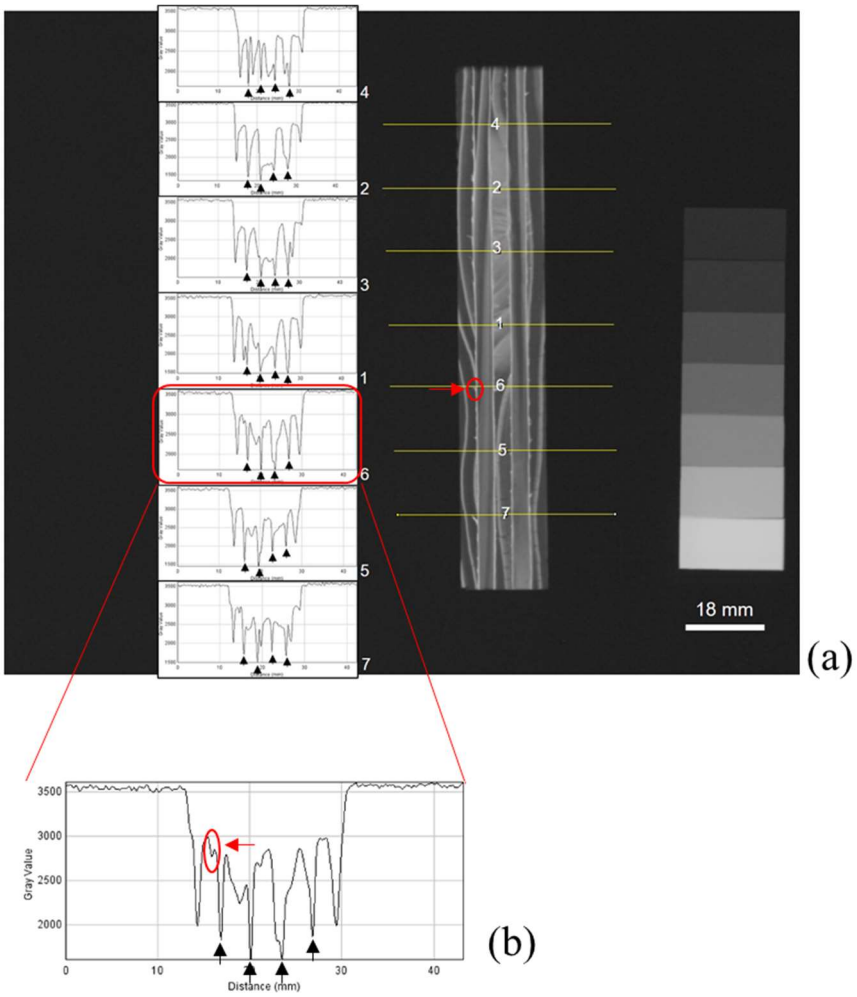

Figure 3. 3 (a) X-ray image of high-density heartwood plywood plot profile with 225 g/m2 glue spreading rate with seven adhesive plot profile with the black arrow pointed on the adhesive peak; (b) Lathe check gray value peak pointed by red arrow which separated for adhesive peak.

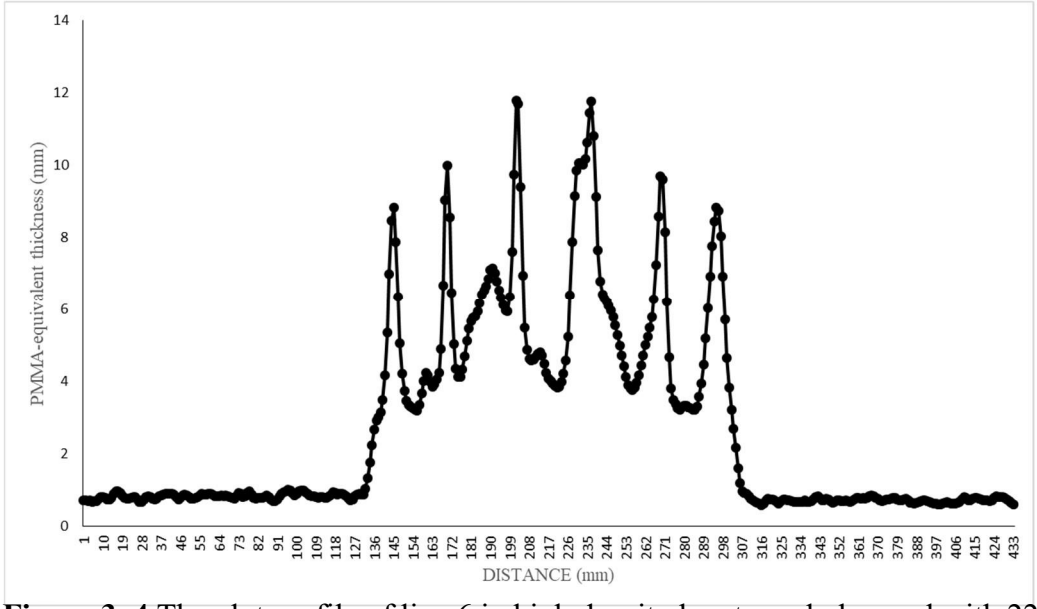

Figure 3. 4 The plot profile of line 6 in high density heartwood plywood with 225 g/cm^2 glue spreading rate that successfully converted using PMMA equation from PMMA calibration curved.

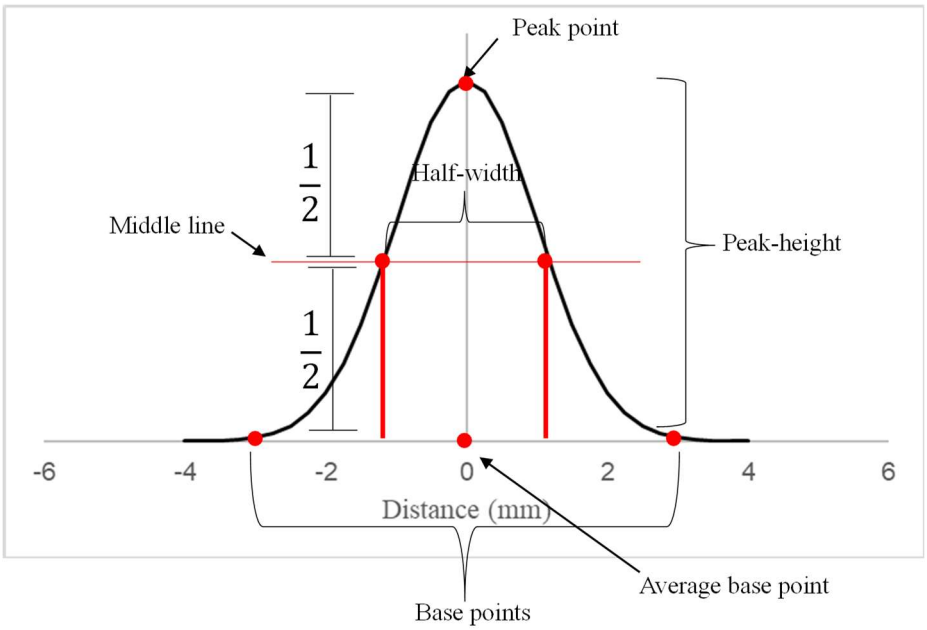

Figure 3. 5 The mechanism of calculated the peak height and half-width

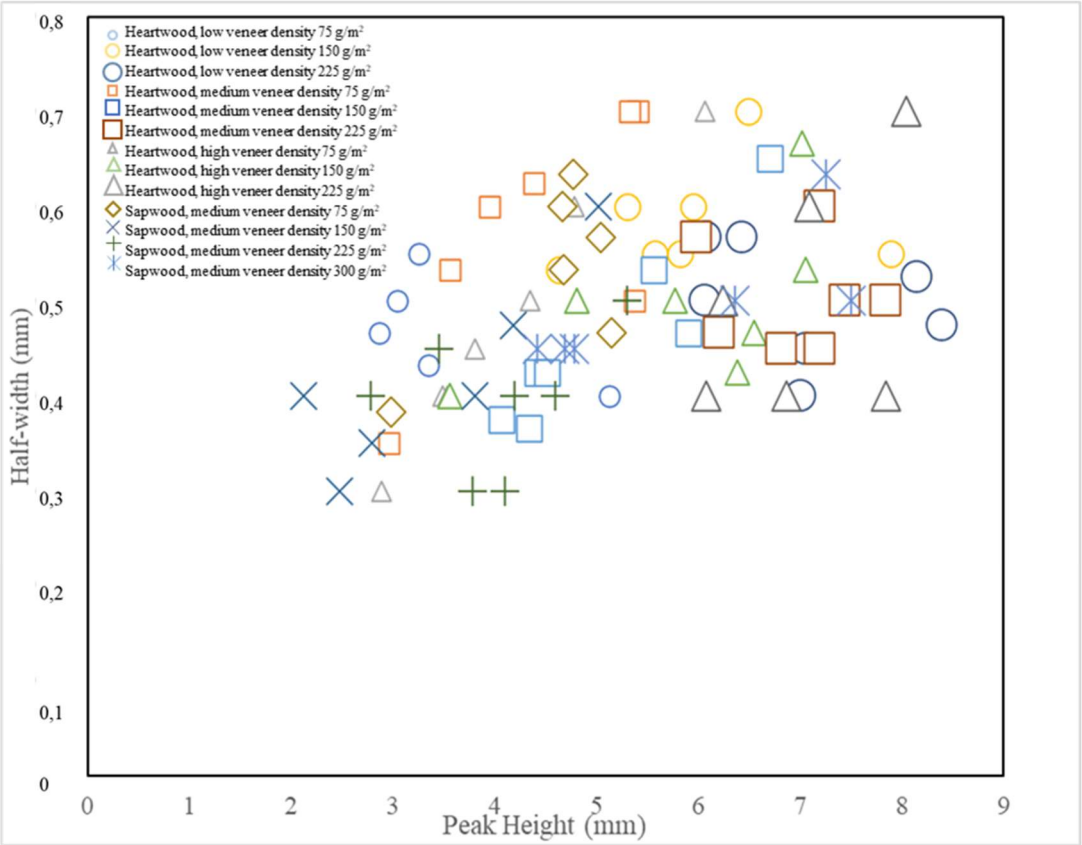

Figure 3. 6 Seven points of peak height and half-width of low, medium, and high veneer density heartwood plywood with 75, 150, 225 g/m^2 glue spreading rate; and medium veneer density sapwood plywood with 75, 150, 225, and 300 g/m^2 glue spreading rate.

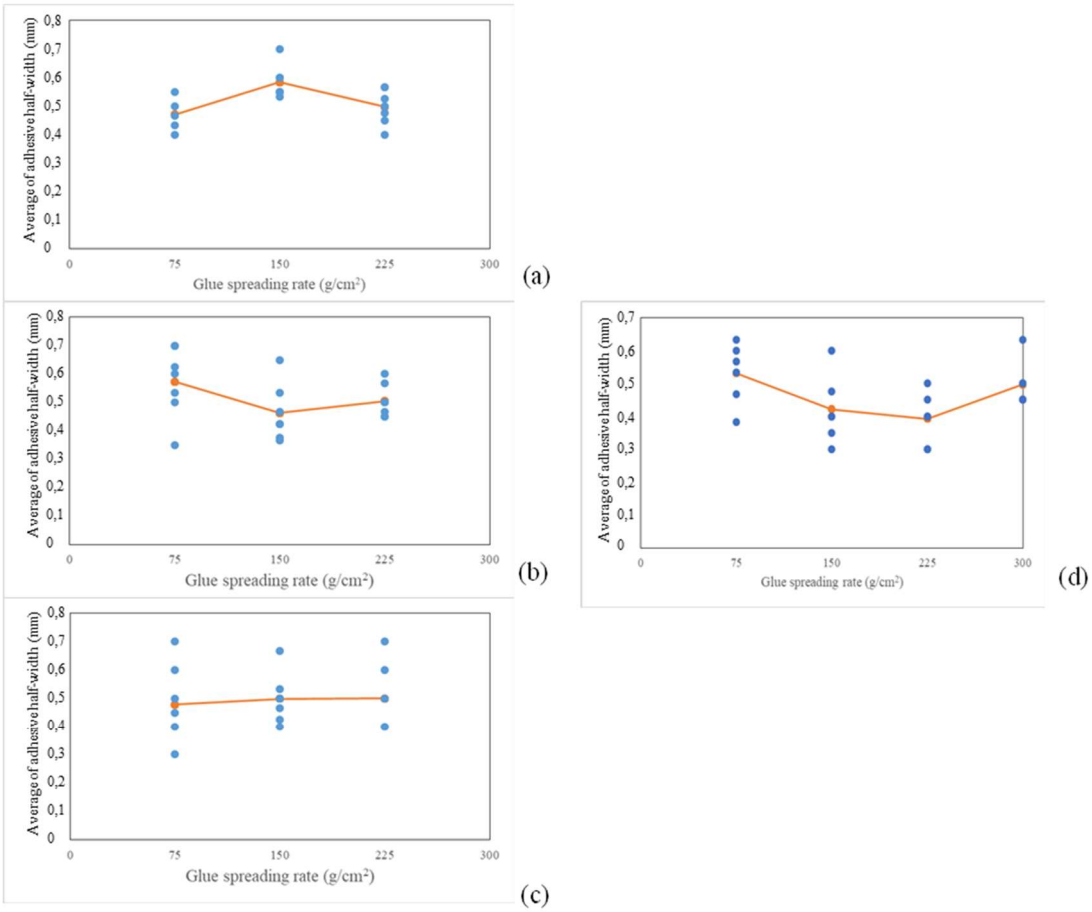

Figure 3. 7 PF adhesive half-width of (a) low density heartwood plywood, (b) medium density heartwood plywood, (c) high density heartwood plywood, and (d) medium density sapwood plywood.

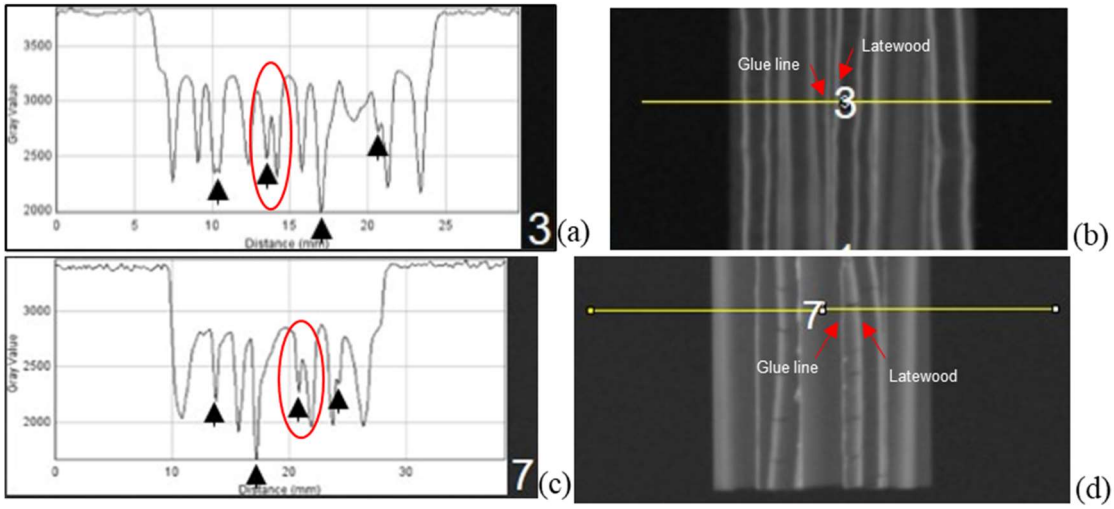

Figure 3. 8 The X-ray image and its plot profile which indicates the smallest half-width value (0.3 mm). (a) A plot profile of medium veneer density of sapwood plywood with 150 g/m^2 glue spreading rate and (b) its X-ray image, and (c) a plot profile of high veneer density of heartwood plywood with 75 g/m^2 glue spreading rate and (d) its X-ray image.

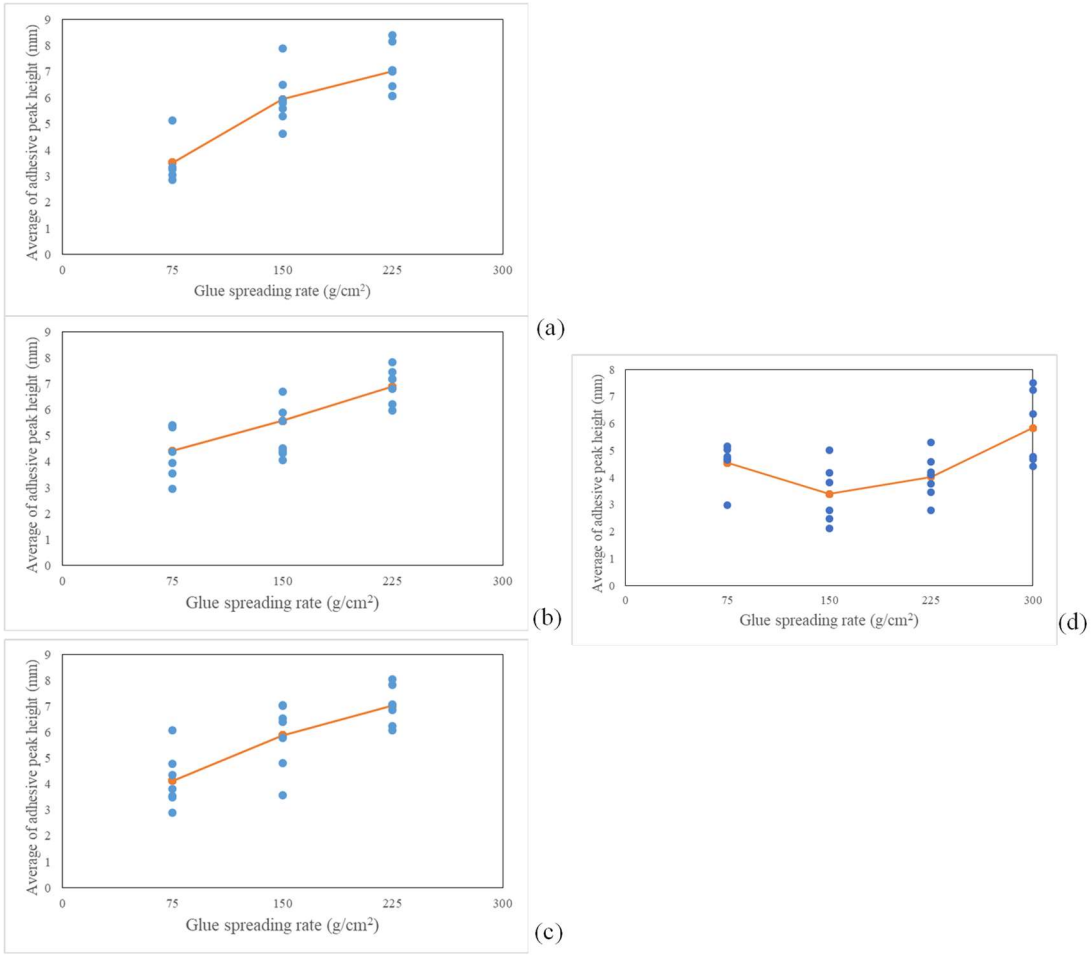

Figure 3. 9 PF adhesive peak height of (a) low density heartwood plywood, (b) medium density heartwood plywood, (c) high density heartwood plywood, and (d) medium density sapwood plywood

CHAPTER 4

THE VISUALIZATION OF LOW-MOLECULE PHENOL (LMP) AND COPPER NAPHTHENATE ON TREATED WOOD USING X-RAY MICROTOMOGRAPHY

4.1 Introduction

The use of X-rays as a non-destructive technique to provide qualitative and quantitative analyses has been extensively researched. Many X-ray methods have been combined and developed to meet the need for evaluating treated wood. Wood is treated to increase its physical properties, and the quality of the treated wood can be evaluated by the spreading (penetration) of the treatment agent/reagent throughout the wood. The specific methods used to examine the micro-distribution of preservative materials using X-ray are energy dispersive analysis (EDX), X-ray fluorescence (XRF) microscopy, and X-ray micro-computed tomography (CT) (Schultz et al., 2014). The use of preservatives increases the density of wood; therefore, X-ray densitometry can be used to inspect the management of wood properties, including wood density after treatment (Taylor and Franklin, 2011). In addition to clearly visualizing the reagent, the mass attenuation of the reagent is also scanned when using X-rays (Tomazello et al., 2008). Organic materials are difficult to visualize because they contain the same chemical as that of the wood itself.

In recent years, the plywood industry has used various hardwood (wood from broad-leaved trees) and softwood (wood from conifer trees) species from industrial forests to be wood veneer (sheet) for their plywood. Those are inferior quality wood that has low density, many defects, weak, and often easily to get attack by fungi and termites (Tanaka et al., 2015). The hardwood species used mostly a fast-growing species such as falcata wood (*Falcataria mollucana* (Miq.) Barneby & J.W. Grimes), Jabon wood (*Anthocephalus cadamba* (Roxb.) Miq), Surian wood (*Toona sinensis* (A.Juss.) M.Roem), Beechwood (*Gmelina arborea*

Roxb.), Manglid wood (*Manglietia glauca* (Blume) Figlar & Noot.), and Rubber wood (*Hevea brasiliensis* (Willd. ex A. Juss.) Müll. Arg.).

Falcata wood is the most popular fast-growing species in tropical country. It is suitable for veneer production with smaller veneer thickness range was 1.95-2.99 mm which led to better physical and mechanical properties of the plywood product. However, the specific gravity of it is low (Mangurai et al. 2018).

The softwood that commonly used for plywood and LVL industry in Japan is Japanese cedar (*Cryptomeria japonica* (L. f.) D. Don). Japanese cedar is ranked as type IV among the common coniferous species of structural timber (National Standards of the Republic of China; CNS 14630, 2017). Japanese cedar has natural antifungal and insect resistant extracts in each heartwood and sapwood part of it. The heartwood contains of essential oil and methanol extracts that had a good inhibitory effect on the activity of wood–decaying fungi and phytopathogen. The sapwood contains hexane soluble which active in resisting vector mosquito larvae (Morita et al., 1997). However, the plywood and LVL manufacturing may change some of the original properties.

The non-wood species that has prospective resource for plywood industry is oil palm (*Elaeis guineensis* Jacq.). The abudant of oil palm trunk, around 9 million trees/ year, has a prospective resource for the plywood industry. However, this prospective material has inferior quality in dimentional stability, low strength, and less durability. According to its anatomy is contains around 50% of soft parenchyma tissue and vascular bundles (Schmidt et al., 2016 and Loh et al., 2011). The Schmidt et al. (2016) investigated the mass loss of oil palm wood by fungus *Coniophora puteana* up to 61%.

Currently, low-molecule phenol (LMP) is often used to improve wood properties (Wang and Chui, 2012) by enhancing its dimensional stability and biological features. Copper naphthenate has also been used to increase veneer durability, particularly for protection of

the veneer surfaces against staining fungi as a wood preservative (Civardi et al., 2016). Appropriate instruments are needed for quality control of the LMP and copper naphthenate treated veneer to determine the distribution of those materials without wasting the tested material.

X-ray microtomography could be a promising method for non-destructive testing to measure and visualize the micro-distribution of LMP and copper naphthenate with high resolution and three-dimensional (3D) images without damaging the wood (Biziks et al., 2016; Van den Bulcke et al., 2013; Paris et al., 2014). X-ray microtomography data can not only determine the distribution of the preservative reagent, but can also map the density of the treated wood and changes to the cell wall (Modzel et al., 2011; Furuno et al., 2004). The penetration phenomena are affected by not only the atomic number of the reagent added to the wood, but also by its concentration, which can be visualized clearly using X-ray microtomography (Gilani et al., 2014).

Although X-ray microtomography is powerful for investigating the inner structure of polymer composite materials, the marginal difference in contrast between carbon-based materials such as petroleum-based plastics or organic materials is still an issue. Therefore, almost all previous studies have conducted the addition of contrast medium or chemical modification of materials before X-ray microtomography (Paris et al., 2014; Modzel et al., 2011; Furuno et al., 2004). The addition or modification, however, is not suitable for industrial use, such as quality control.

More recently, a sub-microscale higher contrast CT apparatus was developed, which is suitable for carbon-based materials and thus can be used for the morphological evaluation of carbon fiber reinforced polymer (CFRP) materials (Garcea et al., 2018). Oishi and Tanaka (2020) have attempted to directly observe adhesive bondlines of plywood and glulam using six X-ray microtomography apparatuses and successfully visualized the wood adhesive at

the bondlines without any addition or chemical modification. In this study, however, the field of view (FOV) was at maximum 3.6 mm ϕ, which is not suitable for industrial applications.

Accordingly, the aim of this study was to determine the applicability of X-ray microtomography to distinguish nano-anatomical elements of wood (wood cell wall, lumen, among other variables), and the reagents (LMP and Cu) on LMP and copper naphthenate treated-wood using seven wood species. In relation to the quality assessment of the treated product, the penetration phenomena of LMP and Cu in the X-ray image and image plot profile were investigated. In this study, matters related to X-ray microtomography technique such as larger FOV, best image contrast quality for scientific morpho-anatomy analysis, simplicity of technique ensuring that the sample being scanned was without additives and chemical modifications, various wood species, and ingredients of the LMP and copper naphthenate material were checked.

4.2 Materials and methods

4.2.1 Specimen preparation

Six Indonesian hardwood species, one Japanese softwood species, and one non-wood species were used in this experiment. The rotary veneer of those wood was cut with dimensions of 100 mm^2 (Fig. 4. 1). Five rotary veneers were prepared for each wood species. One was prepared as a control (no chemical treatment to enhance the wood quality), three were prepared as LMP impregnating treatment sample, and one was prepared as copper naphthenate dipping sample. The physical properties of the reagents (LMP and copper naphthenate) are listed in Table 4. 1.

4.2.2 Low molecule phenol (LMP) impregnating treatment

Three rotary veneers of seven wood species and one non-wood species were impregnated with LMP (Fig. 4. 2). The impregnation pressure of the LMP was maintained at 5 kg/cm^2 for 30 min using a Krisbow KW20-425 pump (Fig. 4. 2c,d). After treatment, all veneers were oven-dried at 103 °C for 15 h. The veneer density and weight percentage gain were calculated using Eqs. (1) and (2), respectively, and are presented in Table 4. 2.

$$\boldsymbol{\rho} = \frac{\boldsymbol{mass\ (g)}}{\boldsymbol{volume\ (cm^3)}} \quad (1)$$

4.2.3 Copper naphthenate dipping treatment

A rotary veneer with dimension of 100 mm^2 of seven wood species and one non-wood species were dipped in copper naphthenate for 1 s (Fig. 4. 3). After treatment, all veneers were oven-dried at 103 °C for 15 h. The veneer density and weight percentage gain were calculated using Eqs. (1) and (2), respectively, and are presented in Table 4. 2.

$$\boldsymbol{weight\ percentage\ gain}\ (\%) = \mathbf{100}\ \% \times \frac{(\boldsymbol{final\ weight\ (g) - initial\ weight\ (g)})}{|\boldsymbol{initial\ weight\ (g)}|} \quad (2)$$

4.2.4 Preliminary study of the visualization of LMP and copper naphthenate treated veneer using X-ray microtomography

4.2.4.1 X-ray specimen preparation

Two X-ray sample test were prepared in this study. One sample was used to understand operating procedure of X-ray apparatus and X-ray setting. The other sample was used to establish an X-ray scanning setting and X-ray image field of view to achieve excellent visualization of LMP and Cu distribution in the treated veneer.

To understand operating procedure of X-ray apparatus and X-ray setting, medium density Sugi sapwood plywood with dimension 10 mm x 100 mm x 17 mm was prepared. To achieve establishment of X-ray scanning setting and X-ray image field of view, preliminary X-ray sample of LMP and copper naphthenate treated veneer was prepared with dimension 20 mm x 100 mm x veneer thickness. The X-ray samples were ordered from the observable window of the apparatus (front) to the back as one untreated-veneer (control), three LMP treated-veneer, and one copper naphthenate treated veneer, respectively.

4.2.4.2 X-ray scanning

Medium density Sugi sapwood plywood was scanned using an X-ray microtomography apparatus (Nano 3DX, Rigaku Corporation, Tokyo, Japan) with a 40 kV tube voltage, 30 mA tube current, sCMOS X-ray detector equipped with L4320 lens, and a copper X-ray target. The acquisition settings were binning 4 (resulting in 17.600 μm/px), 2 s exposure time, angular step at 0.45° (with 400 projections equaling 180° ÷ 400 = 0.45 angular steps), and the distance between the sample and lens was 15 mm.

X-ray samples of falcata wood and rubber wood were scanned using an X-ray microtomography apparatus (Nano 3DX, Rigaku Corporation, Tokyo, Japan) with a 50 kV tube voltage, 24 mA tube current, sCMOS X-ray detector equipped with L4320 lens, and a molybdenum X-ray target (Fig. 4. 4). The acquisition settings were binning 3 (resulting in 13.200 μm/px), 8 s exposure time, angular step at 0.225° (with 600 projections equaling 180° ÷ 600 = 0.3 angular steps), and the distance between the sample and lens was 17 mm.

4.2.5 Study of LMP and Cu distribution on LMP and copper naphthenate treated veneer using X-ray microtomography

4.2.5.1 X-ray specimen preparation

The X-ray sample tests were prepared with dimensions of 10 mm^2 based on the FOV of the apparatus (Lens L4320, FOV, 14 mm × 10 mm, 4.4 μm/pixel). The X-ray samples were ordered from the observable window of the apparatus (front) to the back as copper naphthenate treated-veneer, untreated-veneer (control), and LMP-treated veneer (Fig. 4. 5). The three samples were then tied together with a rubber band. A focus line was drawn 2 cm from the bottom rubber band to indicate the focus point of the scanning object.

4.2.5.2 X-ray scanning

X-ray samples of all species were scanned using an X-ray microtomography apparatus (Nano 3DX, Rigaku Corporation, Tokyo, Japan) with a 50 kV tube voltage, 24 mA tube current, sCMOS X-ray detector equipped with L4320 lens, and a molybdenum X-ray target (Fig. 4. 6). The acquisition settings were binning 2 (resulting in 8.800 μm/px), 8 s exposure time, angular step at 0.225° (with 800 projections equaling 180° ÷ 800 = 0.225 angular steps), and the distance between the sample and lens was 8 mm, which was reported as an appropriate setting for wood-based material observation (Ekaputri et al., 2021). After scanning, we auto-centered the reconstruction image because the sample shifted during the rotation of the X-ray scanning process.

4.2.6 X-ray image analysis

4.2.6.1 Two-dimensional X-ray analysis

The X-ray image stack obtained from each wood species that was scanned after the reconstruction process had 1236 images with a resolution of 1644 × 1644

pixels. These were analyzed using ImageJ 1.48v software to obtain the gray value plot profile, which represents the material distribution in the wood.

4.2.6.2 Three-dimensional X-ray analysis

Further investigation of the distribution of LMP and Cu in the treated veneer compared with the untreated veneer (control) was performed on the 3D X-ray image using VGstudio software. The existence of anomaly image based on higher or lower gray value was observed from all x, y, z axis of 3D X-ray image. The probability of the distribution of LMP and Cu inside the wood vessel was discovered using this 3D X-ray analysis.

4.3 Results and discussion

4.3.1 Wood density and weight percentage gain

The density changes after treatment with LMP increased for all species; however, the density of seven species after copper naphthenate treatment showed no increase. The weight percentage gain of LMP-treated veneer was greater than that of the copper naphthenate treated veneer (Table 4. 2). A possible reason for these differences is the application method used. The impregnation process (vacuum pressure) changed the air inside the wood cell to LMP (Islam et al., 2008), whereas the dipping process for copper naphthenate did not allow the Cu to completely fill the wood; therefore, there was no significant weight gain.

Both of chemical enhancement led to increasing weight percentage gain (WPG %), nevertheless Japanese cedar sapwood treated by LMP resulted higher WPG % than treated by copper naphthenate. It was scientifically approved that high PF resin solid content increasing the weight gain (Shams and Yano 2004; Shams et al, 2005). It was also supported by lower wood veneer density and high porosity of the sapwood veneer sample.

The average value of heartwood veneer density at 0.27 g/cm^3 which different with density of sapwood veneer used in this study. However, the porosity of those was slightly different at 82.43 % in heartwood veneer, and 73.30 % porosity in sapwood veneer. The implication is that the result still supports the research idea to complete the knowledge of wood enhancement using LMP and Cu into Japanese cedar heartwood and sapwood veneer despite further research is needed. These findings suggested that wood enhancing using a low veneer density of Japanese cedar sapwood increasing WPG %.

4.3.2 Evaluation of preliminary study X-ray image of LMP and copper naphthenate treated veneer

The important specification of X-ray microtomography that has to be concern before used were X-ray energy, field of view (FOV), resolution (voxel size), X-ray power, detector speed and its efficiency. The focus important specification of X-ray microtomography in this study was X-ray energy, field of view of the image, and binning value. X-ray energy in this apparatus was called X-ray target. Copper X-ray target used in this study resulted unclear X-ray image than molybdenum X-ray target. Field of view is related with voxel size of the image, higher field of view resulted higher voxel size and vice versa. The L4320 lens provided 14 mm x 10 mm FOV. The sample image did not capture fully because the sample thickness of medium density Sugi sapwood plywood was higher than the FOV (Fig. 4. 7). Binning is a technique which data of adjacent pixel are combined and read out together as a super pixel. Binning value of 2x2 to 8x8 are commonly utilized in microscopy. It's important to remember that 2x2 binning produces a pixel that's four times the size of the original pixel (Müller et al., 2016). Binning values used on medium density Sugi sapwood plywood was binning 4. Hence, the X-ray image was in low quality with many artifacts occurred.

Binning 3 used on LMP and copper naphthenate treated veneer was not clear enough to visualize the falcata and rubber wood sample. The L4320 lens FOV was not able to capture all five-wood veneer in one frame (Fig. 4. 8).

4.3.3 Two-dimensional X-ray image visualization

The LMP and Cu 2D visualization and gray value plot profile distribution is shown in Fig. 4. 10. The distribution of LMP and Cu in the veneer was successfully observed using X-ray microtomography. The LMP was distributed uniformly to a certain degree throughout the veneer, whereas copper naphthenate was mainly present on the surface. The LMP-treated and copper naphthenate-treated samples appeared brighter with higher gray content than the untreated control. Cu was observed owing to its high atomic number. In contrast, although LMP has the same chemical structure as wood, it was still differentiated from the control because of its high concentration. The average gray value plot profile (Table 4. 3) shows that the distribution of LMP is consistently higher than that of the control. It also reveals that the gray value of the surface of the copper naphthenate samples is higher than that of the internal section. The base gray value plot profile was similar for all species. This indicates that X-ray microtomography is suitable for identifying the variation in wood species using the same X-ray settings, and this was indicated for a majority of the wood species. The morphoanatomy of each wood species treated with LMP and copper naphthenate, and the untreated veneer (control) was also successfully visualized in the X-ray image.

Jabon wood and Beechwood (Fig. 10a, f) X-ray images show the differences between the treated and untreated samples. The image of the LMP-treated veneer was the brightest, which is supported by the plot profile that revealed the most peaks for these woods, thereby resulting in a high average gray value (Table 4. 3).

The anatomy of Japanese cedar wood is that of thick latewood (Kitin et al., 2009). The high peak level of gray value in control sample (untreated veneer) is represent latewood. There are many peaks in gray value plot profile of veneer treated by LMP. The latewood peak level of LMP treated veneer higher than latewood peak level in control sample. So that, there is high possible existence of LMP near latewood.

In case of Japanese cedar sapwood veneer, the dense layer and thick-walled cells of latewood made the distribution of brighter white dot represented LMP difficult to be visualize. The distribution of LMP in the latewood was unclear based on the X-ray images (Fig. 4. 10b), although the plot profile showed that the peak of the latewood portion of the treated veneer was higher than that of the control. The white dot represents LMP distribute almost evenly in the veneer. Nevertheless, mostly concentrated on the edge and near the lathe check. This evidence supports the degree of pit aspiration in sapwood part still open or most of the pits were unaspirated. The LMP be able to move to the edge or surface and lathe check of the veneer. The phenomenon was different with LMP distribution in heartwood veneer (Apsari et al., 022). It was visualized evenly in all wood part. Because a large fraction of aspirated pits in heartwood largely effects the difficulties of liquid movement (Siau, 1995; Matsumura et al., 2005).

The Surian wood X-ray image had many objects in the image (Fig. 4. 10c) because of the octahedral silica that lines the rays (Darwis et al., 2012); therefore, a region dominated by gray color was expected on the X-ray image near the rays that displayed a silica octahedron.

In the Falcata wood (Fig. 10d, e), a bright point is concentrated in the wood vessel of the LMP-treated veneer, which indicates the presence of the reagent. Regarding the anatomy of Falcata wood, the pore (trachea) is clearly visible and can be easily distinguished in the X-ray image. The main observation with this wood was the reduction in the size of the

treated veneer compared with the untreated veneer (control), which was related to the LMP infusion (Fig. 4. 10e).

Rubber wood from community and industrial forests differed in their anatomy, and this was successfully observed in the X-ray microtomography images, as shown in Fig. 4. 10g, h. The evidence of tyloses that are common in rubber wood vessels can be seen clearly on the untreated veneer (control) of the sample from the community forest (Fig. 4. 10g), whereas the existence of prismatic crystals can be observed in the control of samples from the industrial forest (Fig. 4. 10h).

Based on the average gray value, rubber wood from the community forest and Manglid wood treated with copper naphthenate showed higher gray values than wood treated with LMP (Table 4. 3). The plot profile also revealed the highest peak on the surface of the copper naphthenate treated-veneer (Fig. 4. 10g, i).

The 2D image of oil palm show the shrinking and swelling phenomena happened in the treated veneer compare with the size of the untreated veneer. The micro distribution of LMP mostly in the parenchyma of the LMP treated veneer, and seem distributed evenly in the veneer. The brightness level almost same for all part according to the gray value peak in the plot profile. The micro distribution of the Cu in the copper naphthenate treated veneer can be seen from the brightest color of the vascular bundle's border in the copper naphthenate treated veneer (Fig. 4. 9l).

The X-ray image show clearly the swelling phenomenon of the parenchyma in the LMP treated oil palm veneer, and the shrinking phenomenon of parenchyma in the copper naphthenate treated oil palm veneer. The probability of LMP and Cu as the reagent distributed in the treated oil palm veneer can be seen from the peak of the gray value plot profile. The treated veneer has many higher peaks (higher gray value) than the peak of untreated oil palm veneer. The average gray value of copper naphthenate treated veneer was

the highest (18900.15441), followed by LMP treated veneer (17973.6965), and the lowest was the untreated veneer's average gray value (15566.27132).

The anatomy of the oil palm different with the anatomy of wood. The oil palm anatomy contains of vascular bundle and parenchyma. The oil palm also has crystalline silica in the parenchyma. The observation from X-ray image stack in 3D form show the existence of the crystalline silica in both treated veneer and untreated veneer (Fig. 4. 10m). The parenchyma of oil palm has <20% klason lignin that contaminated with crystalline silica (Tomimura, 1992).

4.3.4 Three-dimensional X-ray image visualization

The use of 3D image analysis is a convenient way to track the LMP and Cu inside the treated wood, especially in the vessel sections (transverse, radial, and tangential sections). The preliminary analysis can enable identification of the reagent by combining the image stacks to form a 3D visual and by providing a review of the transverse, radial, and tangential sections.

Figure 4. 10 shows one of the 3D images obtained using Manglid wood. The blue, green, and red layers indicate the active 2D image on the transverse section, the radial section, and the tangential section, respectively. The LMP and Cu in the vessel can be verified based on the intersection of the three sections. This discovery can induce further segmentation steps and calculations that clarify the penetration phenomena and quantitative analyses.

4.4 Conclusions

X-ray microtomography can be used to visualize LMP and Cu in treated wood. The same X-ray microtomography setting is relevant for observing the LMP and Cu in species with different types of wood (hardwood and softwood). The X-ray images show unique

phenomena of the treated wood based on the morpho-anatomy of each wood species. Size changes were observed in the treated wood samples, and the tyloses, octahedral crystal, and silica in certain varieties, and the LMP and Cu materials concentrated in the wood vessel were successfully visualized in 2D and 3D images. The average gray value from the plot profile can quantitatively describe the distribution of LMP and Cu in the treated wood to assess the quality related to the uniformity and heterogeneity of the distribution. The visualization is more focused on smaller samples, Mo X-ray targets, and smaller FOV lenses with high binning settings. The results described here were provided by the non-destructive technique of visualization using X-ray microtomography, which is a powerful and promising method to observe woody materials and reagents in treated wood for quality control in industrial applications.

Table 4. 1 The physical properties of low-molecule phenol (LMP) and copper naphthenate

LMP		Copper naphthenate	
Specifications	Value	Specifications	Value
Molecular weight	< 400	Nonvolatile (%)	80
pH	12	Viscosity (Cps)	285
Viscosity (P)	3.5	Specific gravity	0.998
Specific gravity	1.14	Metal Content (%)	8
Solid content (%)	27.11		

Table 4. 2 The density and weight percentage gain of the low-molecule phenol and copper naphthenate (Cu) treated veneers and untreated veneer (control)

Species name	Treatment	Oven dried density (g/cm^3)	Density after treatment (g/cm^3)	Weight percentage gain (%)
Japanese cedar heartwood *Cryptomeria japonica* (L. f.) D. Don	Control	0.27	-	-
	LMP	0.26	0.43	63.16
	Cu	0.27	0.28	2.56
Japanese cedar sapwood *Cryptomeria japonica* (L. f.) D. Don	Control	0.43	-	-
	LMP	0.40	0.57	43.20
	Cu	0.40	0.41	1.91
Falcata wood from Sumedang city *Falcataria moluccana* (Miq.) Barneby & J.W. Grimes	Control	0.27	-	-
	LMP	0.25	0.38	51.40
	Cu	0.25	0.25	1.69
Falcata wood from Jambi city *Falcataria moluccana* (Miq.) Barneby & J.W. Grimes	Control	0.25	-	-
	LMP	0.28	0.39	37.83
	Cu	0.22	0.23	2.61
Rubber wood from Sumedang city *Hevea brasiliensis* (Willd. ex A. Juss.) Müll. Arg.	Control	0.64	-	-
	LMP	0.60	0.75	25.75
	Cu	0.63	0.64	0.47
Rubber wood from Jambi city *Hevea brasiliensis* (Willd. ex A. Juss.) Müll. Arg.	Control	0.68	-	-
	LMP	0.70	0.85	21.14
	Cu	0.64	0.65	0.69
Jabon wood from Sumedang city *Anthocephalus cadamba* (Roxb.) Miq	Control	0.29	-	-
	LMP	0.35	0.50	43.99
	Cu	0.29	0.29	1.63
Jabon wood from Jambi city *Anthocephalus cadamba* (Roxb.) Miq	Control	0.44	-	-
	LMP	0.50	0.65	29.32
	Cu	0.39	0.41	3.64
Surian wood *Toona sinensis* (A.Juss.) M.Roem	Control	0.41	-	-
	LMP	0.43	0.50	16.53
	Cu	0.42	0.42	0.71
Beechwood *Gmelina arborea* Roxb.	Control	0.42	-	-
	LMP	0.50	0.58	16.22
	Cu	0.42	0.42	0.00
Manglid wood *Manglietia glauca* (Blume) Figlar & Noot.	Control	0.62	-	-
	LMP	0.51	0.63	23.56
	Cu	0.58	0.58	0.72
Oil palm	Control	0.63	-	-
	LMP	0.66	0.87	31.00
	Cu	0.67	0.67	1.03

Table 4. 3 Average gray value differences of all hardwood, softwood, and non-wood species

Species name	Average gray value		
	Control	LMP	Cu
Japanese cedar heartwood	18,555.73	21,443.93	19,785.43
Japanese cedar sapwood	15,795.95	17,058.99	16,494.28
Falcata wood from Sumedang city	17,436.26	18,902.41	16,762.45
Falcata wood from Jambi city	9,178.57	11,731.48	9,478.11
Rubber wood from Sumedang city	14,507.30	15,226.38	15,520.58
Rubber wood from Jambi city	15,749.64	17,488.68	15,655.63
Jabon wood from Sumedang city	13,513.15	15,692.20	14,775.80
Jabon wood from Jambi city	13,953.24	14,588.87	14,127.86
Surian wood	11,934.19	12,250.29	12,082.27
Beechwood	12,807.04	15,215.74	13,149.06
Manglid wood	15,601.04	17,252.75	18,094.21
Oil palm	15,566.27	17,973.70	18,900.15

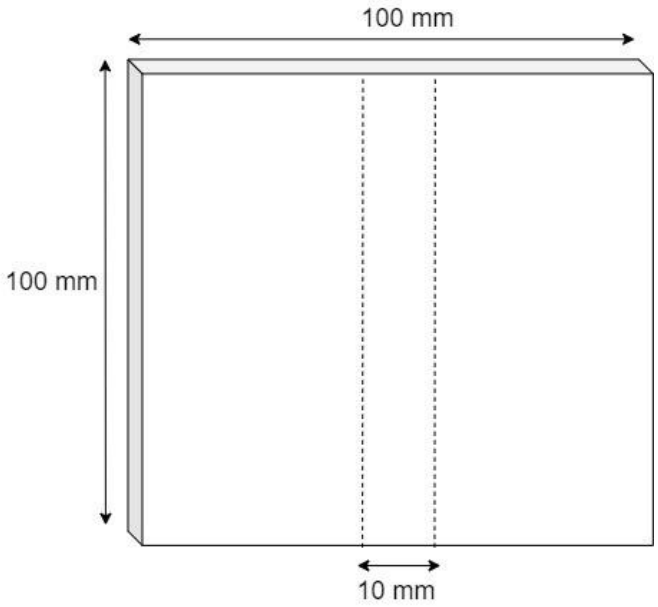

Figure 4. 1 The veneer dimensions used for initial treatment (impregnation of low molecular phenol and dipping of copper naphthenate), and X-ray scanning sample (dashed lines).

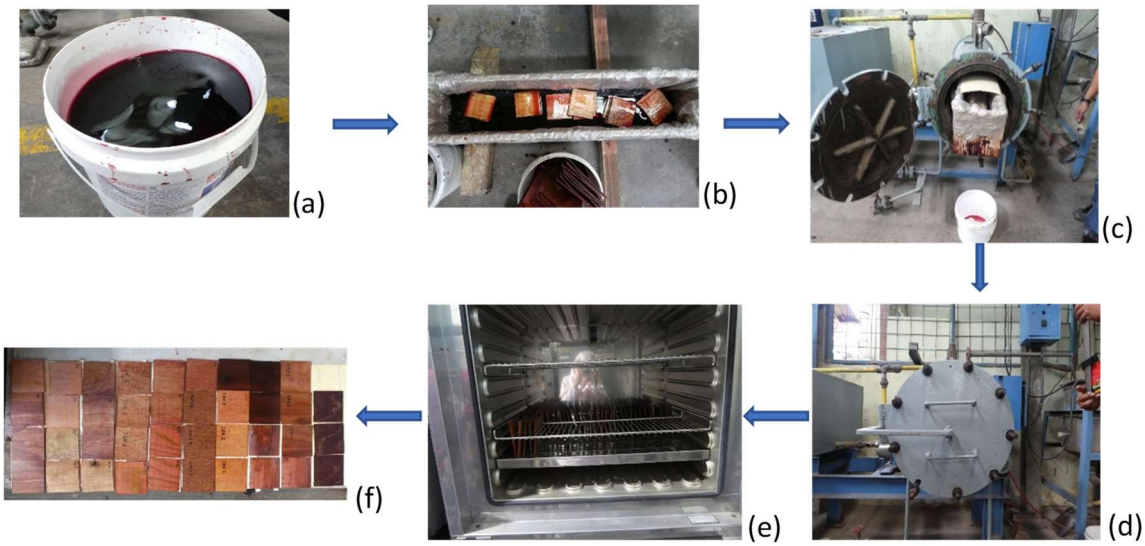

Figure 4. 2 Low molecule phenol (LMP) treatment. (a) LMP liquid; (b) load the veneer sample to LMP liquid into impregnation machine box; (c) put the box into impregnation machine; (d) impregnating; (e) oven drying; (f) oven dried LMP treated-veneer.

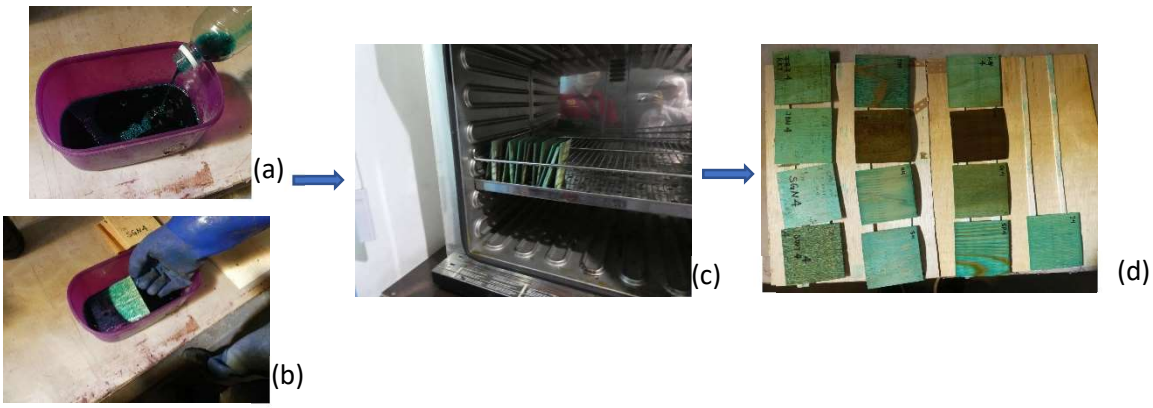

Figure 4. 3 Copper naphthenate (Cu) treatment. (a) copper naphthenate liquid; (b) dipping the veneer sample into copper naphthenate liquid; (c) oven drying; (d) oven dried copper naphthenate treated-veneer

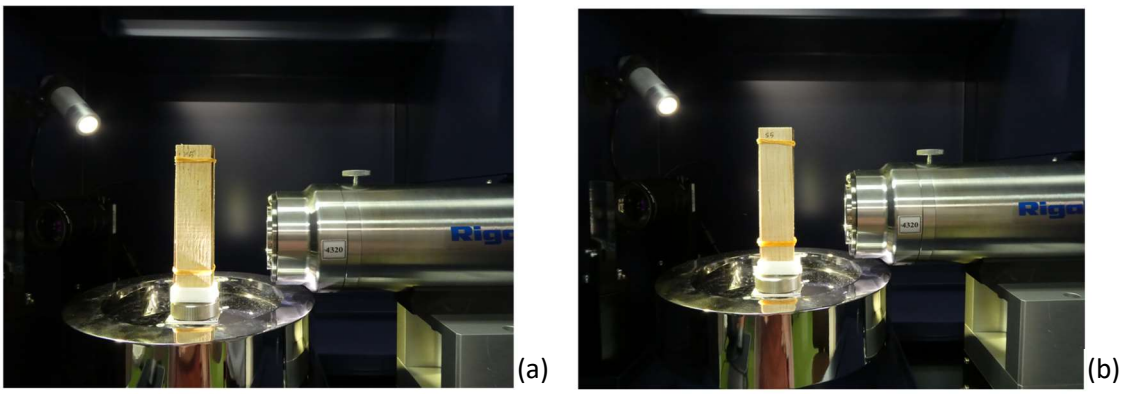

Figure 4. 4 The first X-ray sample dimension of (a) rubber wood and (b) falcata wood to achieve establishment of X-ray scanning setting and X-ray image field of view.

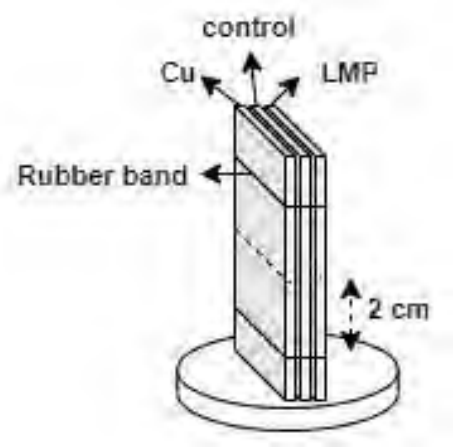

Figure 4. 5 X-ray sample arrangement

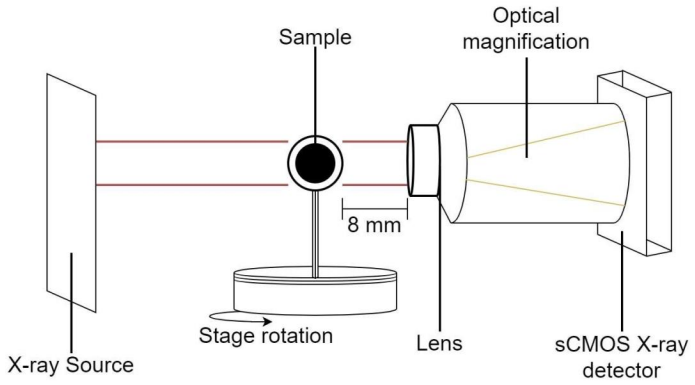

Figure 4. 6 Schematic of the X-ray microtomography apparatus

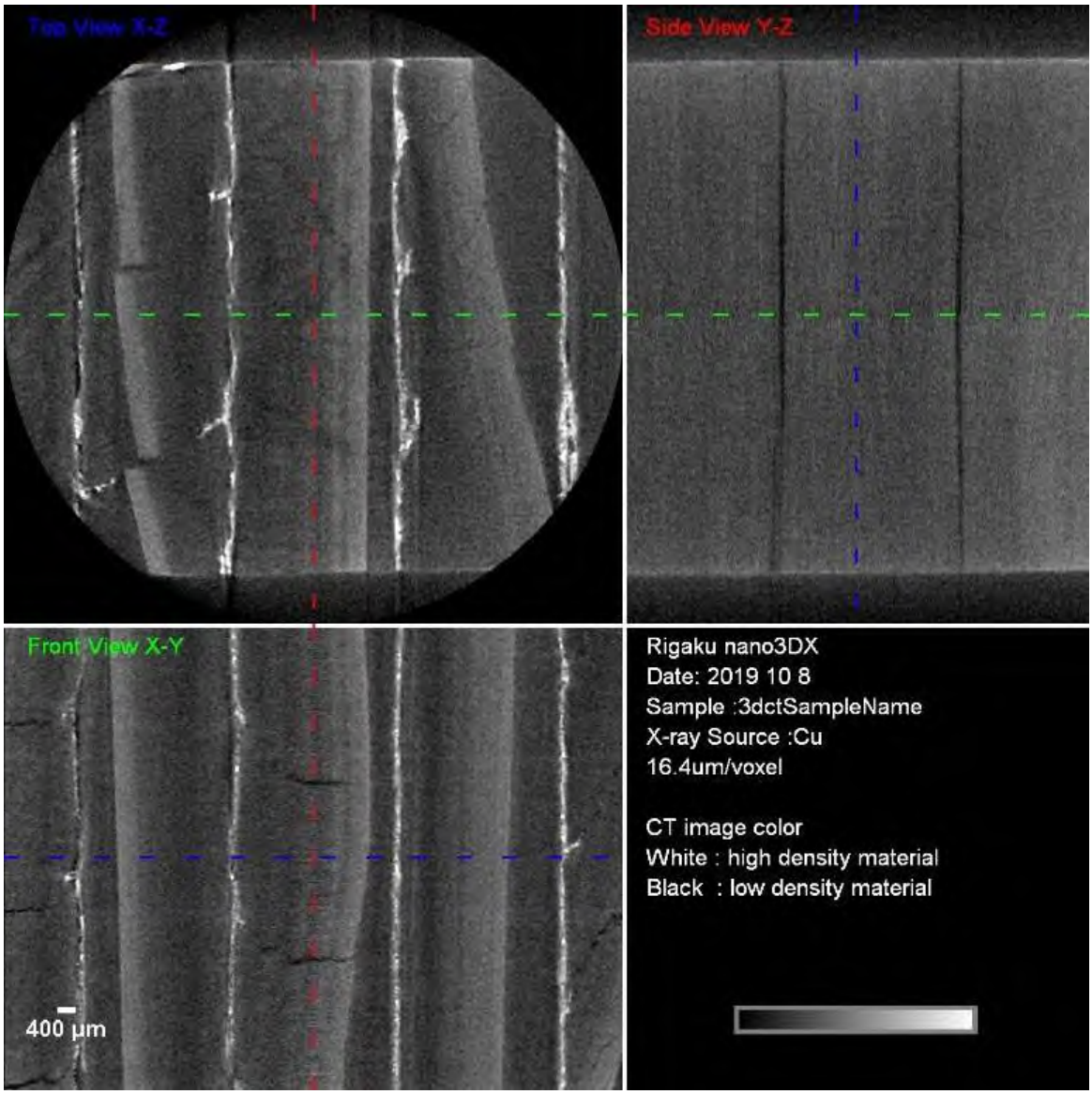

Figure 4. 7 X-ray image of medium density sugi sapwood plywood

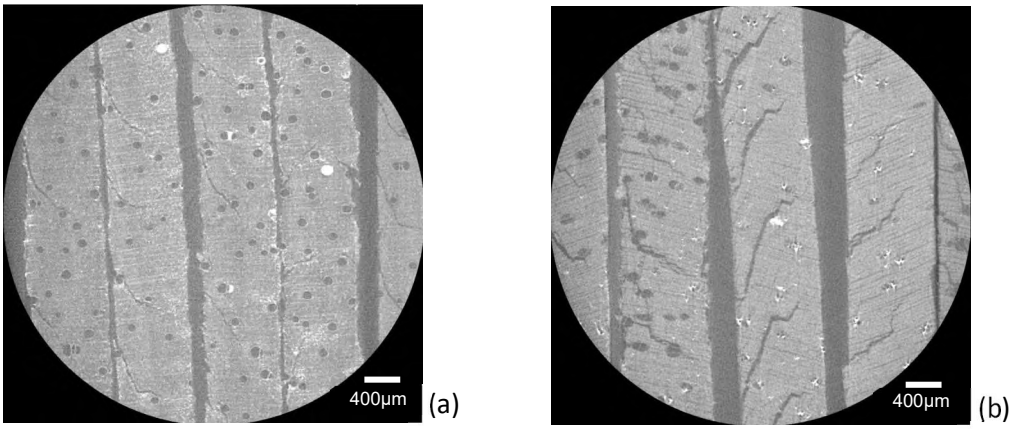

Figure 4. 8 X-ray image (a) falcata wood and (b) rubber wood

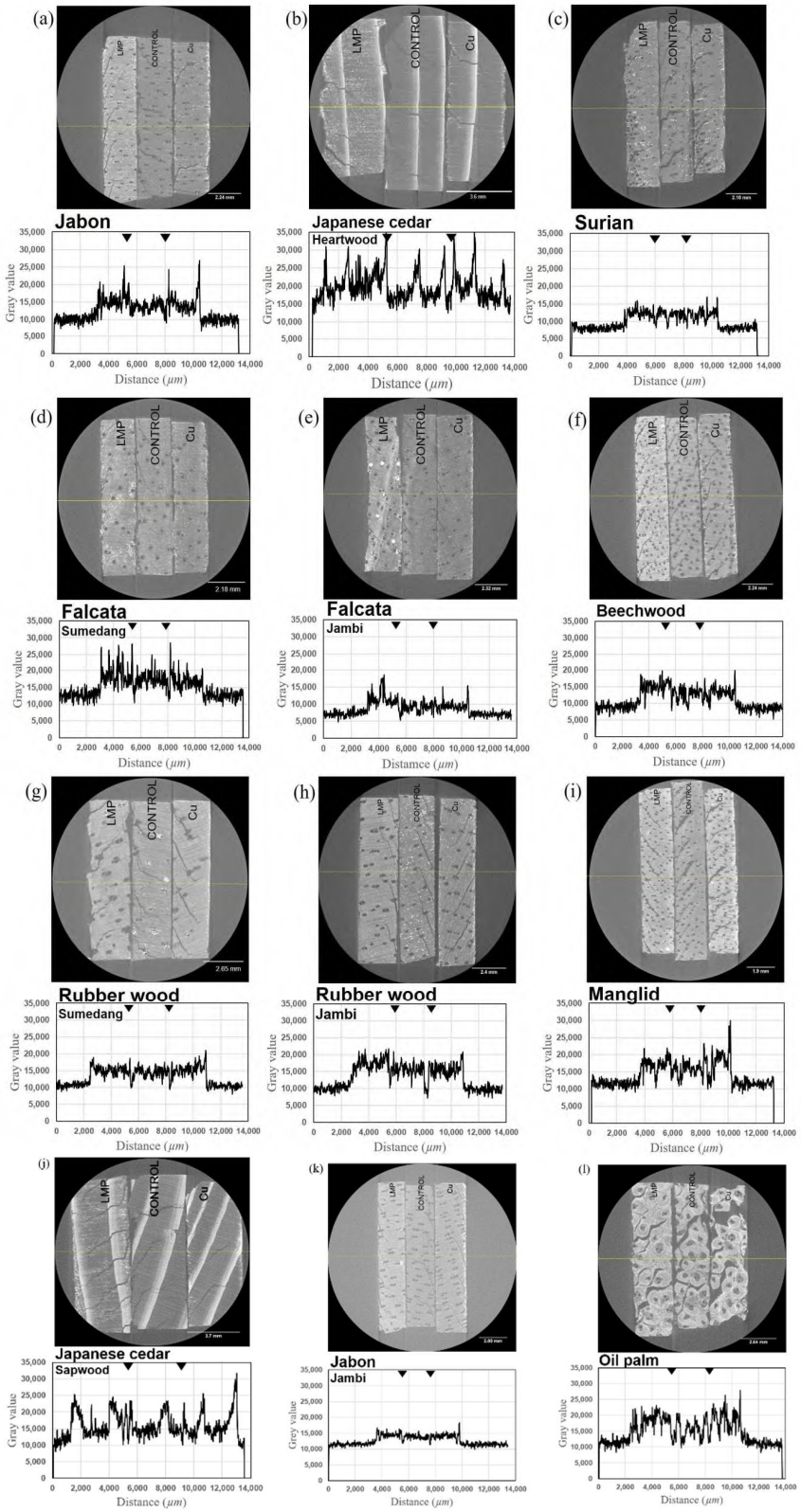

Figure 4. 9 The 2D X-ray visualization of various woods. (a) Jabon wood from Sumedang city, (b) Japanese cedar heartwood veneer, (c) Surian wood, (d) Falcata wood from Sumedang city, (e) Falcata wood from Jambi city, (f) Beechwood, (g) Rubber wood from Sumedang city, (h) Rubber wood from Jambi city, and (i) Manglid wood, (j) Japanese cedar sapwood veneer, (k) Jabon wood from Jambi city, (l) Oil palm including the image gray value of the yellow middle line.

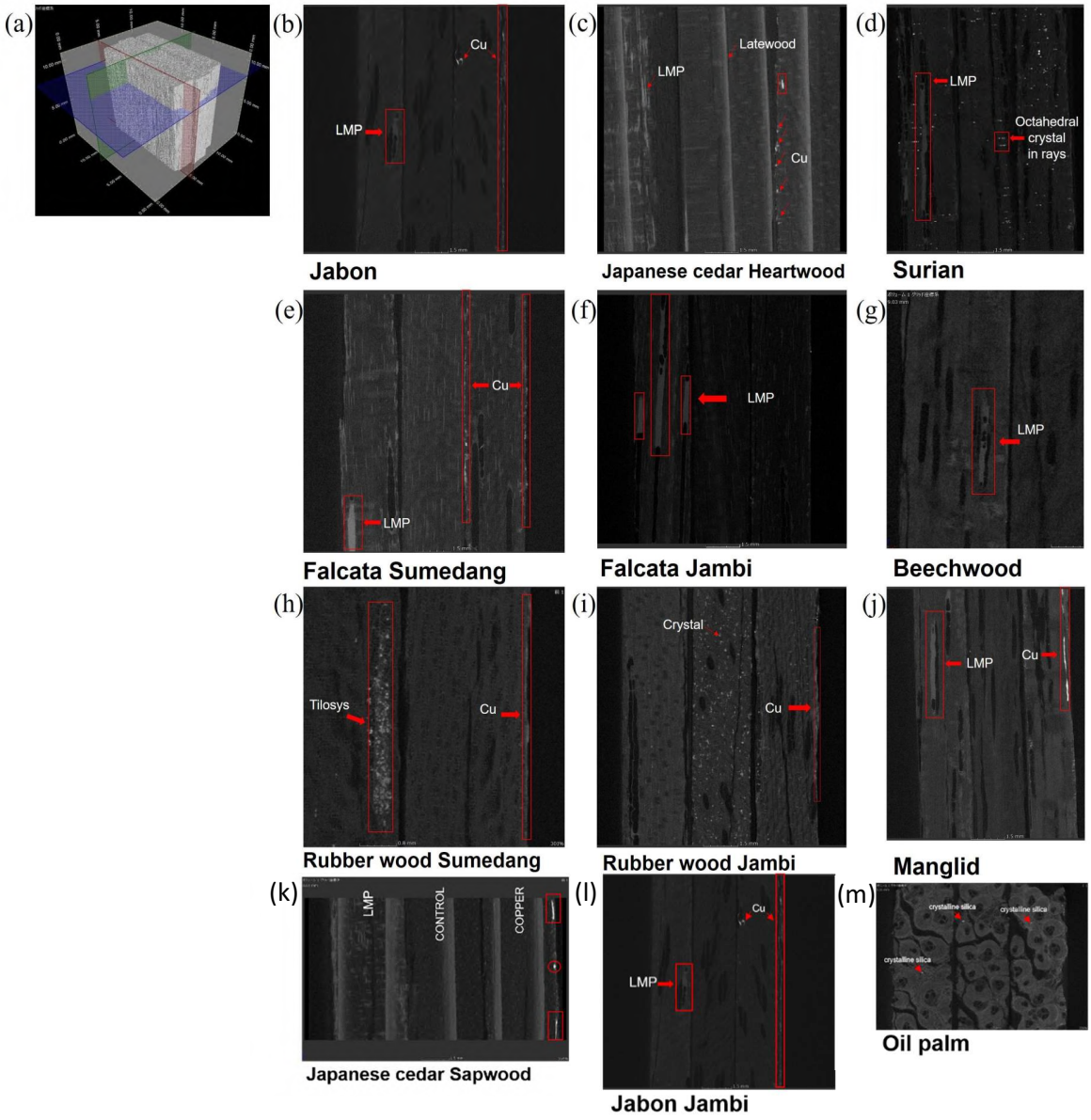

Figure 4. 10 A 3D X-ray observation of the distribution of LMP and Cu, (a) A 3D image stack of the treated-veneer by LMP and copper naphthenate, and the untreated veneer; softwood and hardwood 2D representative images of a radial section that obtained from the green cut section of the 3D image (b) Jabon wood from Sumedang city, (c) Japanese cedar heartwood veneer, (d) Surian wood, (e) Falcata wood from Sumedang city, (f) Falcata wood from Jambi city, (g) Beechwood, (h) Rubber wood from Sumedang city, (i) Rubber wood from Jambi city, (j) Manglid wood, (k) Japanese cedar sapwood, (l) Jabon from Jambi city, and (m) oil palm.

CHAPTER 5

GENERAL CONCLUSIONS

The basic material to produce plywood is wood veneer. A wood product that made from wood veneers glued together with their grains in a perpendicular direction is called plywood. This study has two different research which related into one wood product called plywood. Each research has its own main objective related to wood quality determination. It determines thorough visualization which adopt non-destructive technique to do it. It is because efficiency of testing sample persuades plywood industry and wood resources.

The X-ray apparatus was choosing as non-destructive technique to visualize morpho-anatomical phenomena on plywood and wood veneer to produce plywood. The A conventional simple roentgen X-ray was used to investigate the effect of increasing glue spreading rate, different wood veneer density, and wood part (heartwood and sapwood part) on the half-width size which define as adhesive penetration into wood. X-ray microtomography was used to investigate LMP and copper distribution into wood in two- and three-dimensional X-ray image. Using a conventional simple roentgen X-ray, the method to calculate half-width was developed. Using recent advance X-ray microtomography which used to investigate more than one wood species was provided X-ray setting establishment to investigate material distribution into wood.

First research finding regarding relationship between PF adhesive penetration and the effect of increasing glue spreading rate, different wood veneer density, and wood part (heartwood and sapwood part) was shows a positive result. The method to calculate half-width which define as PF adhesive penetration (resin-rich region) was also developed. The finding shows that the concentration profile of sugi plywood with a low X-ray tube voltage was successfully evaluated. The PF adhesive penetration in the sugi plywood had values of

0,3–0,9 mm, with an average of 0,5 mm. In this experiment, using sugi plywood, it was shown that the existence of latewood might limit the PF adhesive penetration. On the other hand, the PF adhesive concentration in the glue line increases with increasing veneer density and glue spreading rate. Findings from this study would be useful in the analysis of a plywood's quality and durability.

Second research finding regarding the applicability of X-ray microtomography to visualize LMP and copper distribution into wood was shows a positive result. The same X-ray microtomography setting is relevant for observing the LMP and Cu in species with different types of wood (hardwood and softwood) and non-wood material. The X-ray images applicable to show unique phenomena of the treated wood based on the morpho-anatomy of each wood species. The probability of the tyloses, octahedral crystal, and silica in certain varieties, and the LMP and copper materials concentrated in the wood vessel were successfully visualized in two- and three-dimensional images. The average gray value from the plot profile can quantitatively describe the distribution of LMP and Cu in the treated wood to assess the quality related to the uniformity and heterogeneity of the distribution. The visualization is more focused on smaller samples, Mo X-ray targets, and smaller FOV lenses with high binning settings. The results described here were provided by the non-destructive technique of visualization using X-ray microtomography, which is a powerful and promising method to observe woody materials and reagents in treated wood for quality control in industrial applications.

REFERENCES

A. J Stamm, R. M. Seborg. Resin-treated wood (Impreg). Report 1380, Madison, U.S.D.A., Forest Service, F P.L., 1962 (revised)

Asif M. 2009. 2-Sustainability of timber, wood and bamboo in construction. In: Sustainability of construction materials. Khatib JM (ed), Woodhead Publishing, Sawston, United Kingdom. https://doi.org/10.1533/9781845695842.31

Biziks, V. et al. Various Instrumental Methods for Quantifying Phenol-Formaldehyde Resin into Beech Wood. [Conference presentation abstract]. 12th Annual Meeting of the Northern European Network for Wood Science and Engineering WSE, Riga, Latvia. https://biblio.ugent.be/publication/8587476/file/8587478.pdf

Civardi, C. et al. Penetration and effectiveness of micronized copper in refractory wood species. *PLoS ONE* 11, e0163124. https://doi.org/10.1371/journal.pone.0163124 (2016).

Cognard P. 2005. 2-Technical characteristics and testing methods of adhesives and sealants. In: Handbook adhesive and sealants. Cognard P (ed), 1 Elsevier, Oxford, United Kingdom. https://doi.org/10.1016/S1874-5695(02)80003-3

Darwis, A., Wahyudi, I. & Damayanti, R. Struktur anatomi kayu surian (Toona sinensis Roem) (Anatomical structure of surian wood (*Toona sinensis* Roem)). *J. Ilmu dan Teknologi Kayu Tropis*. 10, 159–167. https://doi.org/10.51850/jitkt.v10i2.115.g111 (2012).

Ekaputri, T. S., Apsari, A. N. & Tanaka, T. Visualization of commercial coating penetration into Fagus crenata blume wood using a non-destructive X-ray microtomography. *Coatings* 11, 927. https://doi.org/10.3390/coatings11080927 (2021).

Ferrtikasari, N., Tanaka, T., Yamada, M. 2019. Relationship between thermal conductivity and adhesive distribution of phenol-formaldehyde visualized with x-ray computed tomography on sugi (Cryptomeria japonica D.Don) heartwood plywood. In: IOP Conference Series: Materials Science and Engineering, Volume 593, The 14th Pacific Rim Bio-Based Composites Symposium 29–31 October 2018, South Sulawesi Province, Indonesia. http://dx.doi.org/10.1088/1757-899X/593/1/012003

Fisher RC, Tasker HS 1940. The detection of wood boring insects by means of X-rays. Annals Applied Biology 27(1):92-100

Frihart CR (2009) Adhesive groups and how they relate to the durability of bonded wood. J Adhes Sci Technol 23(4):601-617.

Furuno T, Goto T (1978) Structure of the interface between wood and synthetic polymer (XI). The role of polymer in the cell wall on the dimensional stability of wood-polymer composite (WPC). Mokuzai Gakkaishi 24(5):287–293

Furuno T, Goto T (1979) Structure of the interface between wood and synthetic polymer (XII). Distribution of styrene polymer in the cell wall of wood-polymer composite (WPC) and dimensional stability. Mokuzai Gakkaishi 25(7):488–495

Furuno, T., Imamura, Y. & Kajita, H. The modification of wood by treatment with low molecular weight phenol-formaldehyde resin: a properties enhancement with neutralized phenolic-resin and resin penetration into wood cell walls. *Wood Sci. Technol.* 37, 349–361. https://doi.org/10.1007/s00226-003-0176-6 (2004).

Garcea, S. C., Wang, Y. & Withers, P. J. X-ray computed tomography of polymer composites. *Compos. Sci. Technol.* 156, 305–319. https://doi.org/10.1016/j.compscitech.2017.10.023 (2018).

Gilani, M. S., Boone, M. N., Mader, K. & Schwarze, F. W. M. R. Synchrotron X-ray micro-tomography imaging and analysis of wood degraded by *Physisporinus vitreus* and

Xylaria longipes. J. Struct. Biol. 187, 149–157. https://doi.org/10.1016/j.jsb.2014.06.003 (2014).

H.M. Barnes. 2001. Wood: Preservative Treated: Encyclopedia of Materials: Science and Technology.

Imamura H, Okamoto H, Goto T, Yasue Y, Yokota T and Yoshimoto T (1983) Chemistry for wood utilization (in Japanese). Kyoritsu-Shuppan, Tokyo, pp. 261–262

Islam, M. N., Ando, K., Yamauchi, H., Kobayashi, Y. & Hattori, N. Comparative study between full cell and passive impregnation method of wood preservation for laser incised Douglas fir lumber. *Wood Sci. Technol.* 42, 343–350. https://doi.org/10.1007/s00226-007-0168-z (2008).

J. Matsumura, Y. Yamasaki, K. Oda, and Y. Fujisawa, "Profile of bordered pit aspiration in Cryptomeria japonica using confocal laser scanning microscopy: Pit aspiration and heartwood color," J. Wood Sci., vol. 51, no. 4, pp. 328–333, 2005, doi: 10.1007/s10086-004-0668-5.

J. F. SIAU, WOOD: INFLUENCE OF MOISTURE ON PHYSICAL PROPERTIES. 1995.

Jacquin,P., Longuetaud,F., Leban,J.M., and Mothe, F. 2017.X-ray microdensitometry of wood: A review of existing principles and devices. Dendrochronologia, Volume 42, Pages 42-50, https://doi.org/10.1016/j.dendro.2017.01.004.

Jakes, J.E., C.G. Hunt, D.J. Yelle, L.F. Lorenz, K. Hirth, S-C Gleber, S. Vogt, W. Grigsby, and C.R. Frihart. 2015. Synchrotron-based X-ray fluorescence microscopy in conjunction with nanoindentation to study molecular-scale interactions of phenol-formaldehyde in wood cell walls. ACS Applied Materials and Interfaces. 7. pp. 6584-6589. https://doi.org/10.1021/am5087598

Kajita H, Imamura Y (1991) Improvement of physical and biological properties of particleboards by impregnation with phenolic resin. Wood Sci Technol 26(1):63–70

Kitin, P., Fujii, T., Abe, H. & Takata, K. Anatomical features that facilitate radial flow across growth rings and from xylem to cambium in *Cryptomeria japonica. Ann. Bot. London.* 103, 1145–1157. https://doi.org/10.1093/aob/mcp050 (2009).

Kurt, R. 2010. Possibilities of using poplar clones and boron compounds to manufacture fire resistant laminated veneer lumber. In: Project No: 106O556 progress report, Turkish Scientific Research Council, Kavaklıdere / Ankara, TÜRKİYE

Kurt, R., Cil M. 2012. Effect of press pressures on glue line thickness and properties of laminated veneer lumber glued with phenol formaldehyde adhesive. BioResources 7(4): 5346-5354 DOI:10.15376/biores.7.3.4341-4349

Laborie M-PG. 2002. Investigation of the Wood/Phenol-Formaldehyde Adhesive Interphase Morphology. In: PhD Dissertation, Virginia Polytechnic Institute and State University, Virginia, The United State of America.

Lee, M. J., and Copper, P. 2012. Copper Precipitation of Cu-monoethanolamine Preservative in Wood. Holzforschung, Vol. 66, pp. 1017-1024. DOI 10.1515/hf-2012-0014

Loh, Y. F., Paridah, M. T., Hoong, Y. B., and Yoong, A. C. C. (2011). Effects of treatment with low molecular weight phenol formaldehyde resin on the surface characteristics of oil palm (Elaeis quineensis) stem veneer. Materials & Design, Volume 32, Issue 4, Pages 2277-2283. https://doi.org/10.1016/j.matdes.2010.11.014

Mangurai, S. U. N. M., M. Y. Massijaya, Y. S. Hadi, and D. Hermawan. 2018. "The Physical Characteristics of Oil Palm Trunk and Fast-Growing Species Veneer for Composite-Plywood." *IOP Conference Series: Earth and Environmental Science* 196(1).

MARRA, A. A. 1992. Technology of wood bonding: Prin- ciples in practice, 1 Ed., Van Nostrand Reinhold, New York. Pp. 76–80.

Mckinley, Paige & Kamke, Frederick & Ching, Daniel & Zauner, Michaela & Xiao, Xianghui. (2016). Micro X-ray Computed Tomography of Adhesive Bonds in Wood.

Wood and fiber science: journal of the Society of Wood Science and Technology. 48. 2-16.

Modzel, G., Kamke, F. A. & De Carlo, F. Comparative analysis of wood adhesive bondline. *Wood Sci. Technol.* 45, 147–158 (2011).

Morita, S. I., T. Hidaka, and M. Yatagai 1997 Antifungal components of the extractives of Yakusugi. *Mokuzai Hozon* (Wood Protection), 23(2): 61–69

Morrell, J. J. 2018. Chapter 17 - Protection of Wood-Based Materials: Handbook of Environmental Degradation of Materials (Third Edition). William Andrew Publishing, Pages 343-368,https://doi.org/10.1016/B978-0-323-52472-8.00017-4

Müller, C., Greb, C., and Schwab, K. (2016, April 19). *Definition of Basic Technical Terms for Digital Microscope Cameras and Image Analysis*. Leica Microsystems. https://www.leica-microsystems.com/science-lab/definitions-of-basic-technical-terms-for-digital-microscope-camera-and-image-analysis/

Nicholas P. Cheremisinoff, Paul E. Rosenfeld. 2010. Chapter 1 - Wood-preserving chemicals:Handbook of Pollution Prevention and Cleaner Production,Pages 1-26,https://doi.org/10.1016/B978-0-08-096446-1.10001-2.

Oishi, A. & Tanaka, T. Development of a nondestructive imaging method for morphological characterization of adhesive bondlines in wood-based materials using x-ray micro-computed tomography. *J. Adhes. Soc. Japan* 57, 145–151 (2020).

Open-source Java image processing program (ImageJ 1.48v). 2014. Retrieved from http://imagej.net/

Paris, J. L., Kamke, F. A., Mbachu, R. & Gibson, S. K. Phenol formaldehyde adhesives formulated for advanced x-ray imaging in wood-composite bondlines. *J. Mater. Sci.* 49, 580–591. https://doi.org/10.1007/s10853-013-7738-2 (2014).

Ryu JY, Takahashi M, Imamura Y, Sato T (1991) Biological resistance of phenol-resin treated wood. J Jpn Wood Res Soc 37(9):852–858

Scheikl, M. 2002. Properties of the glue line – Microstructure of the glue line. In: Wood Adhesion and Glued Products: Glued Wood Products State of the Art Report, Johansson, C. J., Pizzi, T., and Van Leemput, M. (eds.), COST Action E13, 109-111. http://users.teilar.gr/~mantanis/E13-Wood-Adhesion.pdf.

Schmidt, O., Bahmani, M., Koch, G., Potsch, T., and Brandt, K. (2016). Study of the fungal decay of oil palm wood using TEM and UV techniques. International Biodeterioration & Biodegradation, Volume 111, Pages 37-44. https://doi.org/10.1016/j.ibiod.2016.04.014

Schultz, T. P., Goodell, B., & Nicholas, D. D. *Deterioration and Protection of Sustainable Biomaterials* (Chapter 13) 227–238 (2014). https://doi.org/10.1021/bk- 2014-1158.ch013

Tanaka, T. 2018. Simple geometrical model of thermal conductivity and bound-water diffusion coefficient in resin-rich regions of softwood plywood. Wood Sci Technol 52, 331–342 (2018). https://doi.org/10.1007/s00226-018-0985-2

Tanaka, T., Adachi, K. & Yamada, M. X-ray mass attenuation coefficients for some common wood adhesives in the tube voltage range from 15 kV to 100 kV. *Mokuzai Gakkaishi*. 61, 308–315. https://doi.org/10.2488/jwrs.61.308 (2015).

Tanaka, T., Shida, S. 2012. Changes of Through-thickness Moisture Distribution in Wood and Wood-based Materials in Adsorption Phase III. Nondestructive measurement of moisture content distribution in plywood and sheathing insulation fiberboards. Mokuzai Gakkaishi Vol. 58, No.5, p. 271-278. https://doi.org/10.2488/jwrs.58.271

Taylor, A., & Franklin, J. Are fast-grown trees of low quality? A primer on tree growth, wood properties and the value of wood products. The University of Tennessee Institute of Agriculture. Extension publication, 1–5 (2011).

Tomazello, M. et al. Application of x-ray technique in nondestructive evaluation of eucalypt wood. *Maderas Cienc Tecnol*. 10, 139–149. https://doi.org/10.4067/S0718-221X200800 0200006(2008).

Van den Bulcke, J. et al. Potential of X-ray computed tomography for 3D anatomical analysis and micro densitometrical assessment in wood research with focus on wood modification. *Int. Wood Prod J.* 4, 183–190. https://doi.org/10.1179/2042645313Y.0000000046 (2013).

Wang, B. J. & Chui, Y. H. Performance evaluation of phenol formaldehyde resin impregnated veneers and laminated veneer lumber. *Wood Fiber Sci*. 44, 5–13 (2012).

White M.S. 1975. Influence of Resin Penetration on the Fracture Toughness of Bonded Wood. In: PhD Dissertation, Virginia Polytechnic Institute and State University, Virginia, The United State of America.

Worschitz F 1932. L'utilization des rayos. In: Congrès IUFRO, X en vue de l'etude de la qualité du bois Paris. France, pp 459–489 (In France)

ACKNOWLEDGMENTS

In the first place, I sincerely thank the Almighty Allah for His mercies, power, provision, and, most importantly, for His faithfulness and love throughout my academic career up to this doctoral level. His kindness has enabled me to succeed and flourish in all of my academic endeavors.

My sincere gratitude is due to my kind, encouraging, and modest supervisor, Assoc. Prof. Kenji KOBAYASHI, for all of his important guidance and contributions throughout my studies. Prof., I treasure your advice and kind words because they more than illuminate my way. In the course of our research, I greatly appreciate your support and high level of independence. The support and contributions of my nimble, friendly, and full of excellent research idea co-supervisor Assist. Prof. Takashi Tanaka. Your words of inspiration and encouragement were incredibly helpful, even during the moments that seemed to be difficult. I appreciate you very much. My unalloyed appreciation goes to my amiable, ever supportive and humble second co-supervisor from Gifu University is Professor Tohru Mitsunaga. Your constructive idea and your humble way of teacher organic chemistry to me was help me develop to be a critical thinking researcher in a good way.

I would like to thank Professor Shingo KAWAI who always gave me his time to discuss my research and PhD life during my PhD program specially in Shizuoka University as my host university to do my research. I'm grateful with warm encouragement you gave to me during my study.

I would like to express my sincere thanks to Assoc. Prof. Eka Mulya Alamsyah as my collaborative advisor from Indonesia. He opened the door for me to continue my study to Japan since I was an undergraduate student 4th grade. Also, I'm very grateful to him for his Indonesian wood materials supply for my research.

I would like to thank the Ministry of Education, Culture, Sport, Science and Technology (MEXT) of Japan for the Japanese government (Monbukagakusho) scholarship, for their financial support and chance to continue my study in Japan.

The impregnating treatment of low molecule phenol (LMP) and copper naphthenate dipping treatment have been performed in PT. Sumber Graha Sejahtera, Sampoerna Kayoe Ltd., Indonesia. My sincere grateful to PT. Sumber Graha Sejahtera "Sampoerna Kayoe" for providing the material and facility for conducting the LMP and copper naphthenate treatments. I gratefully acknowledged. Takeshi Arizono for performing and explaining the LMP and copper naphthenate materials and the applied process. Mr. Eko Sudoyo for giving permission to do collaborative research with biggest plywood industry in Indonesia and help for many documents work relating the collaborative research.

Warm thanks to my lovely junior Ms. Tyana Solichah Ekaputri for big love and support during my hard time doing PhD program. Warm thanks also go to Mr. Kozuka Tetta and Ms. Amano from Shizuoka University faculty of agriculture office for many supports regarding many school documents. I'm very grateful to Mr. YusriFaizal Gumilar Winata, Ms. Yukina Katafuchi and Mr. Idris Maliki for giving many moral supports and help under data analysis and writing the PhD dissertation manuscript and published paper.

The goal of earning a PhD's degree would never have come to my mind without biggest moral support and sacrifice from my family. Especially my mother, Santikawati, who always pushes me up to continue my study to higher education level. This doctoral's dissertation is dedicated for them.

Last but not least, quoting from a song by Snoop Dog, "*...I wanna thank me, I wanna thank me for believing in me, I wanna thank me for doing all this hard work, I wanna thank me for having no days off, I wanna thank me for... for never quitting, I wanna thank me for always being a giver and tryna give more than I receive, I wanna thank me for tryna do more*

right than wrong, I wanna thank me for just being me at all times" . Thank you myself for everything.

SUMMARY

Plywood is a wood product that made from wood veneers glued together with their grains in a perpendicular direction. The most popular adhesive used in plywood industry is phenol formaldehyde adhesive (PF). Optimum adhesive penetration information is important of the efficiency in using the adhesive. Most of the adhesive penetration discussion refers to bonding strength despite environmental aspects that can also be part of the discussion, such as thermal conductivity and bound-water diffusion coefficient. Thus, it is important to investigate the adhesive penetration through the adhesive interphase on plywood.

X-rays can be used to investigate adhesive penetration until microscopic penetration. However, limitation of knowledge regarding the quantitative analysis of adhesive penetration in plywood requires further research. So, research main objective focused to understand whether the half-width size will be in the fixed size or not concerning increasing glue spreading rate, different wood veneer density, and wood part (heartwood and sapwood part). The method to calculate half-width was also developed.

The basic material to produce plywood is wood veneer. Plywood veneer mostly produced from rotary cutting of blocks on a lathe. In recent years, the plywood industry has used various hardwood (wood from broad-leaved trees) and softwood (wood from conifer trees) species from industrial forests to be wood veneer (sheet) for their plywood. Those are inferior quality wood that has low density, many defects, weak, and often easily to get attack by fungi and termites.

The recent plywood industry used low molecule phenol (LMP) to increased wood properties, such as to enhance dimensional stability and biological properties of wood. They also used copper naphthenate to increase their veneer durability, especially to protect veneer surface against staining fungi as a wood preservative. The appropriate instruments are

needed to determine the quality of the LMP and copper naphthenate treated veneer without wasted the testing material, especially to determine the distribution of those material on the treated veneer.

X-rays can be used to investigate material distribution into wood until microscopic penetration. Since the last century, X-ray has been used for wood inspection. A conventional simple roentgen X-ray provide two-dimensional X-ray image only. However, the recent advance X-ray apparatus can provide not only two-dimensional image, but also three-dimensional X-ray image with high quality image which persuade excellent research result. A conventional simple roentgen X-ray was used to investigate the effect of increasing glue spreading rate, different wood veneer density, and wood part (heartwood and sapwood part) on the half-width size which define as adhesive penetration into wood. X-ray microtomography was used to investigate LMP and copper distribution into wood in two- and three-dimensional X-ray image. Using a conventional simple roentgen X-ray, the method to calculate half-width was developed. Using recent advance X-ray microtomography which used to investigate more than one wood species was provided X-ray setting establishment to investigate material distribution into wood.

The PF adhesive penetration research work as explained in Chapter 3 was conducted to understand relationship between half-width size and the effect of increasing glue spreading rate, different wood veneer density, and wood part (heartwood and sapwood part), two-way analysis of variance (ANOVA) was analyzed. Accordingly, the concentration profile of sugi plywood with a low X-ray tube voltage was successfully evaluated. The PF adhesive penetration in the sugi plywood had values of 0,3–0,9 mm, with an average of 0,5 mm. In this experiment, using sugi plywood, it was shown that the existence of latewood might limit the PF adhesive penetration. On the other hand, the PF adhesive concentration in the glue line increases with increasing veneer density and glue spreading rate.

The LMP and copper distribution investigation into wood worked as explained in Chapter 4 was conducted to achieve establishment of X-ray scanning setting to help determine the wood veneer quality after chemical enhancement. The finding shows that the same X-ray microtomography setting is relevant for observing the LMP and Cu in species with different types of wood (hardwood and softwood) and non-wood material. The X-ray images applicable to show unique phenomena of the treated wood based on the morpho-anatomy of each wood species. The probability of the tyloses, octahedral crystal, and silica in certain varieties, and the LMP and Cu materials concentrated in the wood vessel were successfully visualized in 2D and 3D images. The average gray value from the plot profile can quantitatively describe the distribution of LMP and Cu in the treated wood to assess the quality related to the uniformity and heterogeneity of the distribution. The visualization is more focused on smaller samples, Mo X-ray targets, and smaller FOV lenses with high binning settings. The results described here were provided by the non-destructive technique of visualization using X-ray microtomography, which is a powerful and promising method to observe woody materials and reagents in treated wood for quality control in industrial applications.

概要

合板は、木製のベニヤを木目と垂直方向に接着して作られた木製品です。 合板業界で使用される最も人気のある接着剤は、フェノールホルムアルデヒド接着剤（PF）です。 最適な接着剤浸透情報は、接着剤を使用する際の効率にとって重要です。 接着剤の浸透に関する議論のほとんどは、熱伝導率や結合水拡散係数など、議論の一部となる可能性のある環境的側面にもかかわらず、接着強度に言及しています。 したがって、合板上の接着剤中間相を通る接着剤の浸透を調査することが重要です。

X 線を使用して、顕微鏡での浸透まで接着剤の浸透を調べることができます。 ただし、合板への接着剤の浸透の定量分析に関する知識の限界は、さらなる研究が必要です。 そのため、接着剤の散布速度の増加、木製のベニヤ密度の違い、および木材部分（心材と辺材部分）に関して、半幅サイズが固定サイズになるかどうかを理解することに焦点を当てた研究の主な目的があります。 半値幅の計算方法も開発されました。

合板を製造するための基本的な材料は、木製のベニヤです。 合板単板は、主に旋盤でブロックを回転切断して製造されます。 近年、合板業界では、工業林のさまざまな広葉樹（広葉樹からの木材）や針葉樹（針葉樹からの木材）を合板

の単板（シート）として使用しています。 それらは低品質の木材であり、密度が低く、欠陥が多く、弱く、真菌やシロアリに攻撃されやすいことがよくあります。

最近の合板産業では、低分子フェノール（LMP）を使用して、木材の寸法安定性や生物学的特性を強化するなど、木材の特性を向上させています。彼らはまた、ベニヤの耐久性を高めるために、特に木材防腐剤としての真菌の染色からベニヤの表面を保護するために、ナフテン酸銅を使用しました。 LMP およびナフテン酸銅で処理されたベニヤの品質を試験材料を無駄にすることなく決定するには、特に処理されたベニヤ上のこれらの材料の分布を決定するために、適切な機器が必要です。

X 線を使用して、顕微鏡で浸透するまで木材への物質の分布を調べることができます。前世紀以来、X 線は木材検査に使用されてきました。従来の単純なレントゲン X 線は、2 次元の X 線画像のみを提供します。しかし、最近の進歩した X 線装置は、2 次元画像だけでなく、優れた研究結果を納得させる高品質の画像を備えた 3 次元 X 線画像も提供することができます。

従来の単純レントゲン X 線を使用して、接着剤の拡散速度の増加、異なる木製ベニヤ密度、および木材への接着剤の浸透として定義される半幅サイズに対する木材部分（心材および辺材部分）の影響を調査しました。 X 線マイクロトモ

グラフィーを使用して、2 次元および 3 次元の X 線画像で木材への LMP と銅の分布を調査しました。従来の単純レントゲン X 線を使用して、半値幅を計算する方法が開発されました。複数の樹種を調査するために使用された最近の高度な X 線マイクロトモグラフィーを使用して、木材への物質分布を調査するための X 線設定施設が提供されました。

第 3 章で説明した PF 接着剤浸透研究は、半値幅サイズと接着剤拡散率の増加の影響、異なる木製ベニヤ密度、および木材部分（心材と辺材部分）の二元配置分散分析との関係を理解するために実施されました。分散分析（ANOVA）を分析しました。これにより、X 線管電圧の低いスギ合板の濃度プロファイルを評価することに成功しました。スギ合板への PF 接着剤の浸透は、0.3～0.9 mm の値で、平均は 0.5mm でした。この実験では、スギ合板を使用して、晩材の存在が PF 接着剤の浸透を制限する可能性があることが示されました。一方、接着剤ラインの PF 接着剤濃度は、ベニヤ密度と接着剤拡散率の増加とともに増加します。

第 4 章で説明したように機能する木材の LMP と銅の分布調査は、化学的強化後の木製ベニヤの品質を判断するのに役立つ X 線スキャン設定の確立を達成するために実施されました。この調査結果は、同じ X 線マイクロトモグラフィー設定が、異なる種類の木材（広葉樹と針葉樹）と非木材材料の種の LMP と Cu の観

察に関連していることを示しています。各木材種の形態解剖学に基づいて、処理された木材の独特の現象を示すために適用可能な X 線画像。特定の品種のチロース、八面体結晶、およびシリカの確率、および木製の容器に濃縮された LMP および Cu 材料は、2D および 3D 画像で正常に視覚化されました。プロットプロファイルからの平均グレー値は、処理された木材の LMP と Cu の分布を定量的に記述して、分布の均一性と不均一性に関連する品質を評価できます。視覚化は、より小さなサンプル、Mo X 線ターゲット、および高いビニング設定を備えたより小さな FOV レンズに焦点を当てています。ここで説明する結果は、X 線マイクロトモグラフィーを使用した非破壊の可視化手法によって提供されました。これは、工業用途の品質管理のために処理済み木材の木材や試薬を観察するための強力で有望な方法です。

LIST OF PUBLICATIONS CONCERNING THE THESIS

1. Apsari, A.N., Sudoyo, E., Alamsyah, E.M. et al. The visualization of low-molecule phenol (LMP) and copper naphthenate on treated wood using X-ray microtomography. **Sci Rep 12, 2239** (2022). https://doi.org/10.1038/s41598-022-05022-3
2. APSARI, A. N.; TANAKA, T. Effects of glue spreading rate and veneer density on sugi (*Cryptomeria japonica*) plywood adhesive penetration. **Maderas-Cienc Tecnol, [S. l.], v. 25, 2** (2022). Disponível em: http://revistas.ubiobio.cl/index.php/MCT/article/view/5652.

scientific reports

Check for updates

OPEN

The visualization of low-molecule phenol (LMP) and copper naphthenate on treated wood using X-ray microtomography

Ayuni Nur Apsari[1], Eko Sudoyo[2], Eka Mulya Alamsyah[3], Kenji Kobayashi[4] & Takashi Tanaka[4]✉

Recently, the plywood industry has been using low-molecule phenol (LMP) to enhance the dimensional stability of inferior-quality wood, along with copper naphthenate to increase veneer durability against staining fungi as a wood preservative. Non-destructive X-ray microtomography is a promising visualization method for reviewing the distribution of these materials. This study aimed to determine the applicability of X-ray microtomography for observing the distribution of LMP and Cu in two-and three-dimensional visualizations. The distribution mechanisms of these materials were investigated using X-ray images and image plot profiles. Six hardwood (wood from broad-leaved trees) and one softwood (wood from conifer trees) species were used for the experiments. An impregnation process was used to treat the wood samples with LMP, and copper naphthenate was added by dipping the wood in the compound for 1 s. A 10 mm^2 sample of each wood species was scanned using X-ray microtomography, and the distribution of LMP and Cu was successfully visualized using X-ray microtomography with the same settings. The LMP was displayed approximately evenly throughout the veneer, whereas the copper naphthenate existed mainly on the veneer surface. The X-ray images successfully showed penetration at the microscopic scale.

The use of X-rays as a non-destructive technique to provide qualitative and quantitative analyses has been extensively researched. Many X-ray methods have been combined and developed to meet the need for evaluating treated wood. Wood is treated to increase its physical properties, and the quality of the treated wood can be evaluated by the spreading (penetration) of the treatment agent/reagent throughout the wood. The specific methods used to examine the micro-distribution of preservative materials using X-ray are energy dispersive analysis (EDX), X-ray fluorescence (XRF) microscopy, and X-ray micro-computed tomography (CT)[1]. The use of preservatives increases the density of wood; therefore, X-ray densitometry can be used to inspect the management of wood properties, including wood density after treatment[2]. In addition to clearly visualizing the reagent, the mass attenuation of the reagent is also scanned when using X-rays[3]. Organic materials are difficult to visualize because they contain the same chemical as that of the wood itself.

In recent years, the plywood industry has used various hardwood (wood from broad-leaved trees) and softwood (wood from conifer trees) species from industrial forests to be wood veneer (sheet) for their plywood. Those are inferior quality wood that has low density, many defects, weak, and often easily to get attack by fungi and termites[4]. The hardwood species used mostly a fast-growing species such as falcata wood (*Falcataria mollucana* (Miq.) Barneby & J.W. Grimes), Jabon wood (*Anthocephalus cadamba* (Roxb.) Miq), Surian wood (*Toona sinensis* (A.Juss.) M.Roem), Beechwood (*Gmelina arborea* Roxb.), Manglid wood (*Manglietia glauca* (Blume) Figlar & Noot.), and Rubber wood (*Hevea brasiliensis* (Willd. ex A. Juss.) Müll. Arg.). The softwood that commonly used mostly in Japan is Japanese cedar (*Cryptomeria japonica* (L. f.) D. Don).

Currently, low-molecule phenol (LMP) is often used to improve wood properties[5] by enhancing its dimensional stability and biological features. Copper naphthenate has also been used to increase veneer durability, particularly for protection of the veneer surfaces against staining fungi as a wood preservative[6]. Appropriate

[1]The United Graduate School of Agricultural Science, Gifu University, 1-1 Yanagido, Gifu-shi, Gifu 501-1193, Japan. [2]Research and Development Division, PT Sumber Graha Sejahtera, Sampoerna Strategic Square, North Tower, 21st Floor, Jl. Jend. Sudirman Kav. 45-46, Jakarta 12930, Indonesia. [3]Post Harvest Technology Study Program, School of Life Sciences and Technology, Institut Teknologi Bandung, Jalan Ganesha No. 10, Bandung 40132, Indonesia. [4]College of Agriculture, Academic Institute, Shizuoka University, Ohya 836, Suruga-ku, Shizuoka 422-8529, Japan. ✉email: tanaka.takashi@shizuoka.ac.jp

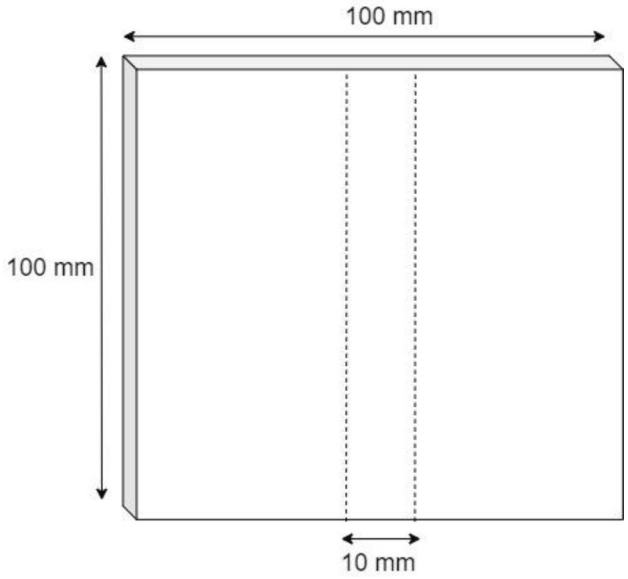

Figure 1. The veneer dimensions used for initial treatment (impregnation of low-molecule phenol and dipping of copper naphthenate), and X-ray scanning sample (dashed lines).

instruments are needed for quality control of the LMP and copper naphthenate treated veneer to determine the distribution of those materials without wasting the tested material.

X-ray microtomography could be a promising method for non-destructive testing to measure and visualize the micro-distribution of LMP and copper naphthenate with high resolution and three-dimensional (3D) images without damaging the wood[7–9]. X-ray microtomography data can not only determine the distribution of the preservative reagent, but can also map the density of the treated wood and changes to the cell wall[10,11]. The penetration phenomena are affected by not only the atomic number of the reagent added to the wood, but also by its concentration, which can be visualized clearly using X-ray microtomography[12].

Although X-ray microtomography is powerful for investigating the inner structure of polymer composite materials, the marginal difference in contrast between carbon-based materials such as petroleum-based plastics or organic materials is still an issue. Therefore, almost all previous studies have conducted the addition of contrast medium or chemical modification of materials before X-ray microtomography[9–11]. The addition or modification, however, is not suitable for industrial use, such as quality control.

More recently, a sub-microscale higher contrast CT apparatus was developed, which is suitable for carbon-based materials and thus can be used for the morphological evaluation of carbon fiber reinforced polymer (CFRP) materials[13]. Oishi and Tanaka have attempted to directly observe adhesive bondlines of plywood and glulam using six X-ray microtomography apparatuses and successfully visualized the wood adhesive at the bondlines without any addition or chemical modification[14]. In this study, however, the field of view (FOV) was at maximum 3.6 mm ϕ, which is not suitable for industrial applications.

Accordingly, the aim of this study was to determine the applicability of X-ray microtomography to distinguish nanatomical elements of wood (wood cell wall, lumen, among other variables), and the reagents (LMP and Cu) on LMP and copper naphthenate treated-wood using seven wood species. In relation to the quality assessment of the treated product, the penetration phenomena of LMP and Cu in the X-ray image and image plot profile were investigated. In this study, matters related to X-ray microtomography technique such as larger FOV, best image contrast quality for scientific morpho-anatomy analysis, simplicity of technique ensuring that the sample being scanned was without additives and chemical modifications, various wood species, and ingredients of the LMP and copper naphthenate material were checked.

Methods

Low-molecule phenol (LMP) and copper naphthenate treatment. Hardwood and Japanese softwood veneers were used in this experiment with sample dimensions of 100 mm^2 (Fig. 1).

Five rotary veneers were prepared for each wood species. One was used as a control (no checimal treatment to enhance the wood quality), three were impregnated with LMP, and one was dipped in copper naphthenate for 1 s. The physical properties of the reagents are listed in Table 1. The impregnation pressure of the LMP was maintained at 5 kg/cm^2 for 30 min using a Krisbow KW20-425 pump. After treatment, all veneers were oven-dried at 103 °C for 15 h. The veneer density and weight percentage gain were calculated using Eqs. (1) and (2), respectively, and are presented in Table 2.

$$\rho = \frac{mass(g)}{volume(cm^3)} \quad (1)$$

LMP		Copper naphthenate	
Specifications	Value	Specifications	Value
pH	12	Nonvolatile (%)	80
Viscosity (P)	3.5	Viscosity (Cps)	285
Specific gravity	1.14	Specific gravity	0.998
Solid content (%)	27.11	Metal content (%)	8

Table 1. The physical properties of low-molecule phenol (LMP) and copper naphthenate.

Species name	Treatment	Oven dried density (g/cm^3)	Density after treatment (g/cm^3)	Weight percentage gain (%)
Japanese cedar heartwood *Cryptomeria japonica* (L. f.) D. Don	Control	0.27	–	–
	LMP	0.26	0.43	63.16
	Cu	0.27	0.28	2.56
Falcata wood from Sumedang city *Falcataria moluccana* (Miq.) Barneby & J.W. Grimes	Control	0.27	–	–
	LMP	0.25	0.38	51.40
	Cu	0.25	0.25	1.69
Falcata wood from Jambi city *Falcataria moluccana* (Miq.) Barneby & J.W. Grimes	Control	0.25	–	–
	LMP	0.28	0.39	37.83
	Cu	0.22	0.23	2.61
Rubber wood from Sumedang city *Hevea brasiliensis* (Willd. ex A. Juss.) Müll. Arg	Control	0.64	–	–
	LMP	0.60	0.75	25.75
	Cu	0.63	0.64	0.47
Rubber wood from Jambi city *Hevea brasiliensis* (Willd. ex A. Juss.) Müll. Arg	Control	0.68	–	–
	LMP	0.70	0.85	21.14
	Cu	0.64	0.65	0.69
Jabon wood from Sumedang city *Anthocephalus cadamba* (Roxb.) Miq	Control	0.29	–	–
	LMP	0.35	0.50	43.99
	Cu	0.29	0.29	1.63
Surian wood *Toona sinensis* (A.Juss.) M.Roem	Control	0.41	–	–
	LMP	0.43	0.50	16.53
	Cu	0.42	0.42	0.71
Beechwood *Gmelina arborea* Roxb	Control	0.42	–	–
	LMP	0.50	0.58	16.22
	Cu	0.42	0.42	0.00
Manglid wood *Manglietia glauca* (Blume) Figlar & Noot	Control	0.62	–	–
	LMP	0.51	0.63	23.56
	Cu	0.58	0.58	0.72

Table 2. The density and weight percentage gain of the low-molecule phenol and copper naphthenate (Cu) treated veneers and untreated veneer (control).

$$\textit{weight percentage gain}\ (\%) = 100\% \times \frac{(\textit{final weight}\ (g) - \textit{initial weight}\ (g))}{|\textit{initial weight}\ (g)|} \tag{2}$$

Sample preparation for X-ray microtomography. The X-ray sample tests were prepared with dimensions of 10 mm^2 based on the FOV of the apparatus (Lens L4320, FOV, 14 mm × 10 mm, 4.4 µm/pixel). The X-ray samples were ordered from the observable window of the apparatus (front) to the back as copper naphthenate treated-veneer, untreated-veneer (control), and LMP-treated veneer (Fig. 2). The three samples were then tied together with a rubber band. A focus line was drawn 2 cm from the bottom rubber band to indicate the focus point of the scanning object.

X-ray microtomography scanning. X-ray samples of all species were scanned using an X-ray microtomography apparatus (Nano 3DX, Rigaku Corporation, Tokyo, Japan) with a 50 kV tube voltage, 24 mA tube current, sCMOS X-ray detector equipped with L4320 lens, and a molybdenum X-ray target (Fig. 3). The acquisition settings were binning 2 (resulting in 8.800 µm/px), 8 s exposure time, angular step at 0.225° (with 800 projections

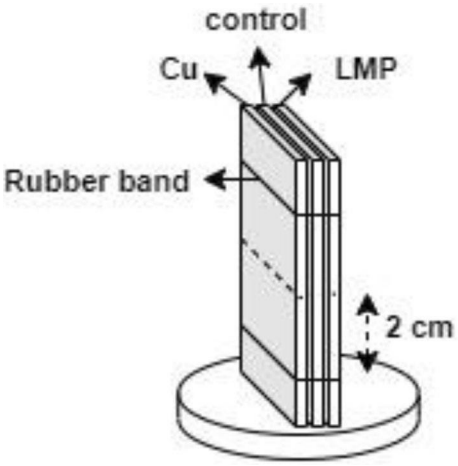

Figure 2. X-ray sample arrangement.

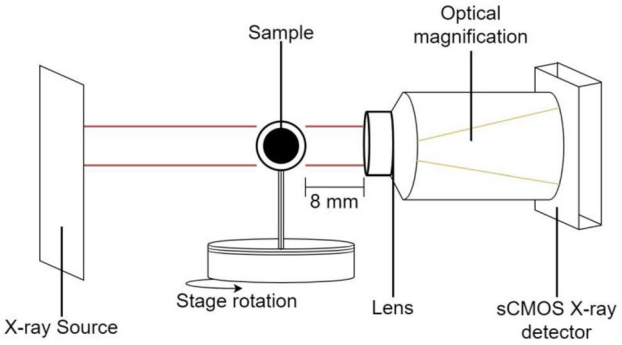

Figure 3. Schematic of the X-ray microtomography apparatus.

equaling 180° ÷ 800 = 0.225 angular steps), and the distance between the sample and lens was 8 mm, which was reported as an appropriate setting for wood-based material observation[15]. After scanning, we auto-centered the reconstruction image because the sample shifted during the rotation of the X-ray scanning process.

X-ray image analysis. The X-ray image stack obtained from each wood species that was scanned after the reconstruction process had 1236 images with a resolution of 1644 × 1644 pixels. These were analyzed using ImageJ 1.48v software to obtain the gray value plot profile, which represents the material distribution in the wood. Further investigation of the distribution of LMP and Cu in the treated veneer compared with the untreated veneer (control) was performed on the 3D X-ray image using VGstudio software.

Results and discussion

Density and weight percentage gain. The density change after treatment with LMP increased for all species; however, the density of seven species after copper naphthenate treatment showed no increase. The weight percentage gain of LMP-treated veneer was greater than that of the copper naphthenate treated veneer (Table 2). A possible reason for these differences is the application method used. The impregnation process (vacuum pressure) changed the air inside the wood cell to LMP[16], whereas the dipping process for copper naphthenate did not allow the Cu to completely fill the wood; therefore, there was no significant weight gain.

2D X-ray image visualization. The LMP and Cu 2D visualization and gray value plot profile distribution are shown in Fig. 4. The distribution of LMP and Cu in the veneer was successfully observed using X-ray microtomography. The LMP was distributed uniformly to a certain degree throughout the veneer, whereas copper naphthenate was mainly present on the surface. The LMP-treated and copper naphthenate-treated samples appeared brighter with higher gray content than the untreated control. Cu was observed owing to its high atomic number. In contrast, although LMP has the same chemical structure as wood, it was still differentiated from the control because of its high concentration. The average gray value plot profile (Table 3) shows that the distribution of LMP is consistently higher than that of the control. It also reveals that the gray value of the surface of the copper naphthenate samples is higher than that of the internal section. The base gray value plot profile was similar for all species. This indicates that X-ray microtomography is suitable for identifying the variation in wood

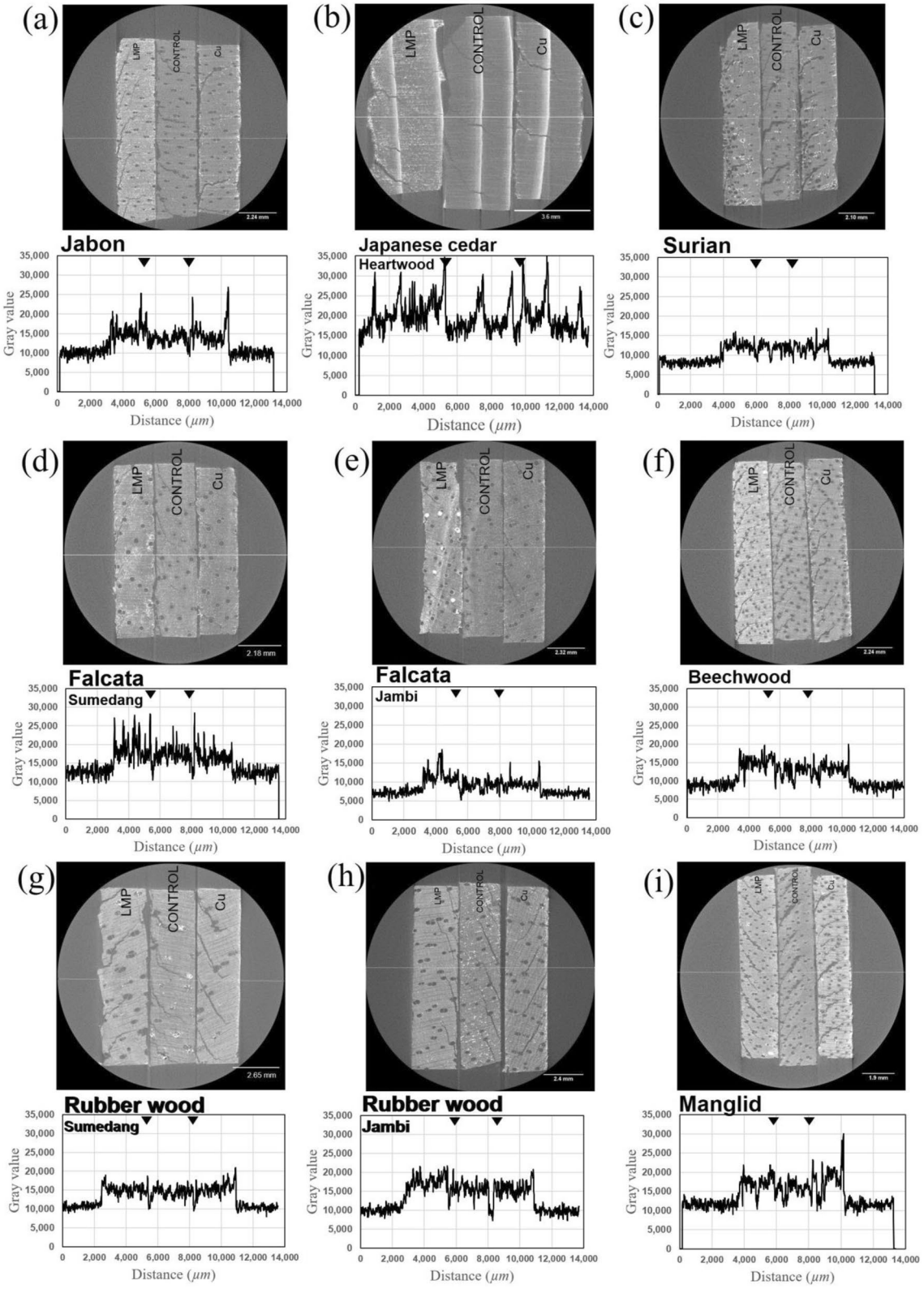

Figure 4. The 2D X-ray visualization of various woods. (**a**) Jabon wood from Sumedang city, (**b**) Japanese cedar heartwood veneer, (**c**) Surian wood, (**d**) Falcata wood from Sumedang city, (**e**) Falcata wood from Jambi city, (**f**) Beechwood, (**g**) Rubber wood from Sumedang city, (**h**) Rubber wood from Jambi city, and (**i**) Manglid wood, including the image gray value of the yellow middle line.

Species name	Average gray value		
	Control	LMP	Cu
Japanese cedar heartwood	18,555.73	21,443.93	19,785.43
Falcata wood from Sumedang city	17,436.26	18,902.41	16,762.45
Falcata wood from Jambi city	9,178.57	11,731.48	9,478.11
Rubber wood from Sumedang city	14,507.30	15,226.38	15,520.58
Rubber wood from Jambi city	15,749.64	17,488.68	15,655.63
Jabon wood from Sumedang city	13,513.15	15,692.20	14,775.80
Surian wood	11,934.19	12,250.29	12,082.27
Beechwood	12,807.04	15,215.74	13,149.06
Manglid wood	15,601.04	17,252.75	18,094.21

Table 3. Average gray value differences of all hardwood, softwood, and non-wood species.

species using the same X-ray settings, and this was indicated for a majority of the wood species. The morpho-anatomy of each wood species treated with LMP and copper naphthenate, and the untreated veneer (control) was also successfully visualized in the X-ray image.

Jabon wood and Beechwood (Fig. 4a, f) X-ray images show the differences between the treated and untreated samples. The image of the LMP-treated veneer was the brightest, which is supported by the plot profile that revealed the most peaks for these woods, thereby resulting in a high average gray value (Table 3).

The anatomy of Japanese cedar wood is that of thick latewood[17]. The distribution of LMP in the latewood was unclear based on the X-ray images (Fig. 4b), although the plot profile showed that the peak of the latewood portion of the treated veneer was higher than that of the control.

The Surian wood X-ray image had many objects in the image (Fig. 4c) because of the octahedral silica that lines the rays[18]; therefore, a region dominated by gray color was expected on the X-ray image near the rays that displayed a silica octahedron.

In the Falcata wood (Fig. 4d, e), a bright point is concentrated in the wood vessel of the LMP-treated veneer, which indicates the presence of the reagent. Regarding the anatomy of Falcata wood, the pore (trachea) is clearly visible and can be easily distinguished in the X-ray image. The main observation with this wood was the reduction in the size of the treated veneer compared with the untreated veneer (control), which was related to the LMP infusion (Fig. 4e).

Rubber wood from community and industrial forests differed in their anatomy, and this was successfully observed in the X-ray microtomography images, as shown in Fig. 4g, h. The evidence of tyloses that are common in rubber wood vessels can be seen clearly on the untreated veneer (control) of the sample from the community forest (Fig. 4g), whereas the existence of prismatic crystals can be observed in the control of samples from the industrial forest (Fig. 4h).

Based on the average gray value, rubber wood from the community forest and Manglid wood treated with copper naphthenate showed higher gray values than wood treated with LMP (Table 3). The plot profile also revealed the highest peak on the surface of the copper naphthenate treated-veneer (Fig. 4g, i).

Preliminary 3D X-ray image analysis. The use of 3D image analysis is a convenient way to track the LMP and Cu inside the treated wood, especially in the vessel sections (transverse, radial, and tangential sections). The preliminary analysis can enable identification of the reagent by combining the image stacks to form a 3D visual and by providing a review of the transverse, radial, and tangential sections.

Figure 5 shows one of the 3D images obtained using Manglid wood. The blue, green, and red layers indicate the active 2D image on the transverse section, the radial section, and the tangential section, respectively. The LMP and Cu in the vessel can be verified based on the intersection of the three sections. This discovery can induce further segmentation steps and calculations that clarify the penetration phenomena and quantitative analyses.

Conclusions

X-ray microtomography can be used to visualize LMP and Cu in treated wood. The same X-ray microtomography setting is relevant for observing the LMP and Cu in species with different types of wood (hardwood and softwood). The X-ray images show unique phenomena of the treated wood based on the morpho-anatomy of each wood species. Size changes were observed in the treated wood samples, and the tyloses, octahedral crystal, and silica in certain varieties, and the LMP and Cu materials concentrated in the wood vessel were successfully visualized in 2D and 3D images. The average gray value from the plot profile can quantitatively describe the distribution of LMP and Cu in the treated wood to assess the quality related to the uniformity and heterogeneity of the distribution. The visualization is more focused on smaller samples, Mo X-ray targets, and smaller FOV lenses with high binning settings. The results described here were provided by the non-destructive technique of visualization using X-ray microtomography, which is a powerful and promising method to observe woody materials and reagents in treated wood for quality control in industrial applications.

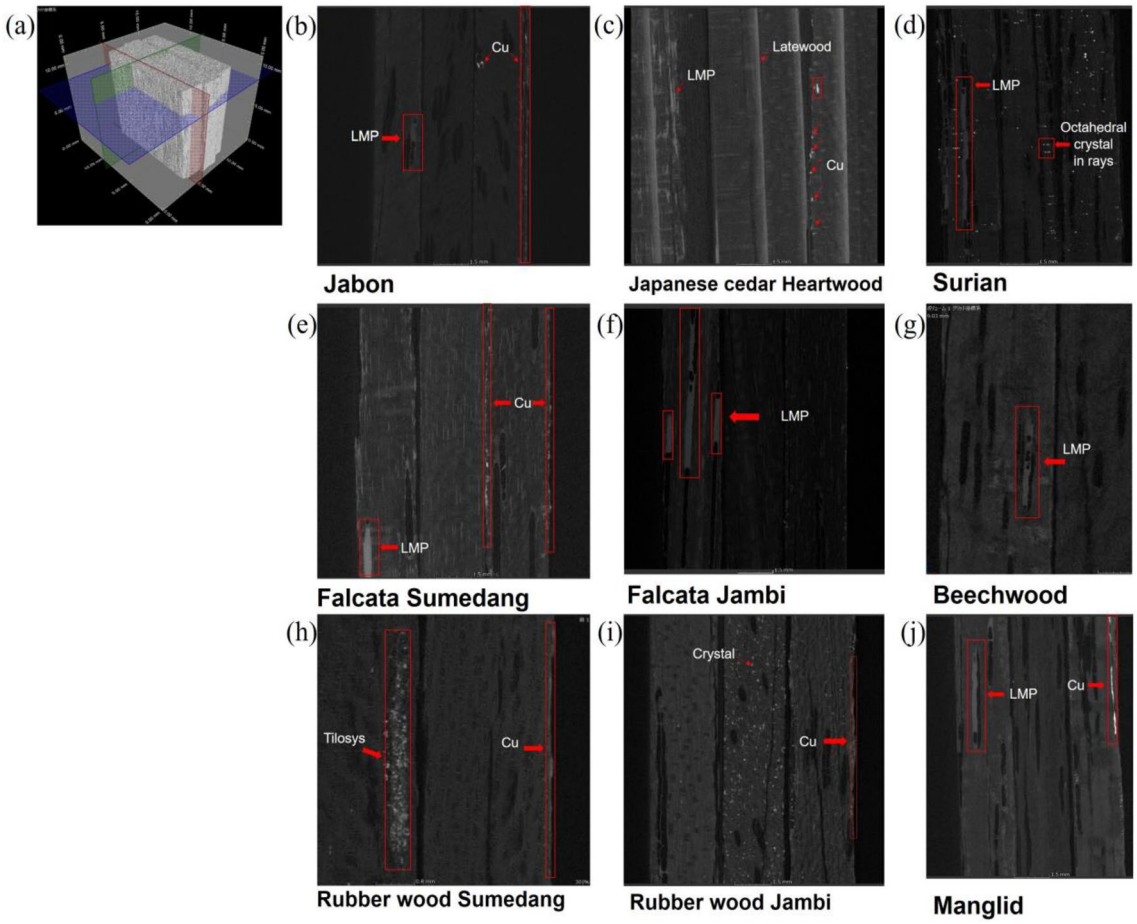

Figure 5. A 3D X-ray observation of the distribution of LMP and Cu. (**a**) A 3D image stack of the treated-veneer by LMP and copper naphthenate, and the untreated veneer; softwood and hardwood 2D representative images of a radial section were obtained from the green cut section of the 3D image, (**b**) Jabon wood from Sumedang city, (**c**) Japanese cedar heartwood veneer, (**d**) Surian wood, (**e**) Falcata wood from Sumedang city, (**f**) Falcata wood from Jambi city, (**g**) Beechwood, (**h**) Rubber wood from Sumedang city, (**i**) Rubber wood from Jambi city, and (**j**) Manglid wood.

Received: 20 August 2021; Accepted: 29 December 2021
Published online: 09 February 2022

References

1. Schultz, T. P., Goodell, B., & Nicholas, D. D. *Deterioration and Protection of Sustainable Biomaterials* (Chapter 13) 227–238 (2014). https://doi.org/10.1021/bk-2014-1158.ch013
2. Taylor, A., & Franklin, J. Are fast-grown trees of low quality? A primer on tree growth, wood properties and the value of wood products. The University of Tennessee Institute of Agriculture. Extension publication, 1–5 (2011).
3. Tomazello, M. *et al.* Application of x-ray technique in nondestructive evaluation of eucalypt wood. *Maderas Cienc Tecnol.* **10**, 139–149. https://doi.org/10.4067/S0718-221X2008000200006 (2008).
4. Tanaka, T., Adachi, K. & Yamada, M. X-ray mass attenuation coefficients for some common wood adhesives in the tube voltage range from 15 kV to 100 kV. *Mokuzai Gakkaishi.* **61**, 308–315. https://doi.org/10.2488/jwrs.61.308 (2015).
5. Wang, B. J. & Chui, Y. H. Performance evaluation of phenol formaldehyde resin impregnated veneers and laminated veneer lumber. *Wood Fiber Sci.* **44**, 5–13 (2012).
6. Civardi, C. *et al.* Penetration and effectiveness of micronized copper in refractory wood species. *PLoS ONE* **11**, e0163124. https://doi.org/10.1371/journal.pone.0163124 (2016).
7. Biziks, V. *et al.* Various Instrumental Methods for Quantifying Phenol-Formaldehyde Resin into Beech Wood. [Conference presentation abstract]. 12th Annual Meeting of the Northern European Network for Wood Science and Engineering WSE, Riga, Latvia. https://biblio.ugent.be/publication/8587476/file/8587478.pdf
8. Van den Bulcke, J. *et al.* Potential of X-ray computed tomography for 3D anatomical analysis and micro densitometrical assessment in wood research with focus on wood modification. *Int. Wood Prod J.* **4**, 183–190. https://doi.org/10.1179/2042645313Y.0000000046 (2013).
9. Paris, J. L., Kamke, F. A., Mbachu, R. & Gibson, S. K. Phenol formaldehyde adhesives formulated for advanced x-ray imaging in wood-composite bondlines. *J. Mater. Sci.* **49**, 580–591. https://doi.org/10.1007/s10853-013-7738-2 (2014).
10. Modzel, G., Kamke, F. A. & De Carlo, F. Comparative analysis of wood adhesive bondline. *Wood Sci. Technol.* **45**, 147–158 (2011).
11. Furuno, T., Imamura, Y. & Kajita, H. The modification of wood by treatment with low molecular weight phenol-formaldehyde resin: a properties enhancement with neutralized phenolic-resin and resin penetration into wood cell walls. *Wood Sci. Technol.* **37**, 349–361. https://doi.org/10.1007/s00226-003-0176-6 (2004).

12. Gilani, M. S., Boone, M. N., Mader, K. & Schwarze, F. W. M. R. Synchrotron X-ray micro-tomography imaging and analysis of wood degraded by *Physisporinus vitreus* and *Xylaria longipes*. *J. Struct. Biol.* **187**, 149–157. https://doi.org/10.1016/j.jsb.2014.06.003 (2014).
13. Garcea, S. C., Wang, Y. & Withers, P. J. X-ray computed tomography of polymer composites. *Compos. Sci. Technol.* **156**, 305–319. https://doi.org/10.1016/j.compscitech.2017.10.023 (2018).
14. Oishi, A. & Tanaka, T. Development of a nondestructive imaging method for morphological characterization of adhesive bondlines in wood-based materials using x-ray micro-computed tomography. *J. Adhes. Soc. Japan* **57**, 145–151 (2020).
15. Ekaputri, T. S., Apsari, A. N. & Tanaka, T. Visualization of commercial coating penetration into *Fagus crenata* blume wood using a non-destructive X-ray microtomography. *Coatings* **11**, 927. https://doi.org/10.3390/coatings11080927 (2021).
16. Islam, M. N., Ando, K., Yamauchi, H., Kobayashi, Y. & Hattori, N. Comparative study between full cell and passive impregnation method of wood preservation for laser incised Douglas fir lumber. *Wood Sci. Technol.* **42**, 343–350. https://doi.org/10.1007/s00226-007-0168-z (2008).
17. Kitin, P., Fujii, T., Abe, H. & Takata, K. Anatomical features that facilitate radial flow across growth rings and from xylem to cambium in *Cryptomeria japonica*. *Ann. Bot. London.* **103**, 1145–1157. https://doi.org/10.1093/aob/mcp050 (2009).
18. Darwis, A., Wahyudi, I. & Damayanti, R. Struktur anatomi kayu surian (*Toona sinensis* Roem) (Anatomical structure of surian wood (*Toona sinensis* Roem)). *J. Ilmu dan Teknologi Kayu Tropis.* **10**, 159–167. https://doi.org/10.51850/jitkt.v10i2.115.g111 (2012).

Acknowledgements

The authors thank JSPS KAKENHI for funding (Fund No.: 20K06163), Takeshi Arizono for performing and explaining the LMP and copper naphthenate materials and the applied process, and PT. Sumber Graha Sejahtera "Sampoerna Kayoe" for providing the material and facility for conducting the LMP and copper naphthenate treatments.

Author contributions

A.N.A. and E.M.A conceived the experiments; A.N.A., E.S., and T.T. conducted the experiments; A.N.A and T.T. analyzed the results; A.N.A. prepared and wrote the original draft; A.N.A and T.T. wrote, reviewed, and edited the manuscript; T.T. and K.K. supervised the research; and T.T. acquired the funding. All authors reviewed the manuscript.

Competing interests

The authors declare no competing interests.

Additional information

Correspondence and requests for materials should be addressed to T.T.

Reprints and permissions information is available at www.nature.com/reprints.

Publisher's note Springer Nature remains neutral with regard to jurisdictional claims in published maps and institutional affiliations.

Maderas-Cienc Tecnol 25(2023):2, 1-17
Ahead of Print: Accepted Authors Version

DOI:10.4067/S0718-221X2023005XXXXXX

EFFECTS OF GLUE SPREADING RATE AND VENEER DENSITY ON SUGI (*Cryptomeria japonica*) PLYWOOD ADHESIVE PENETRATION

Ayuni Nur Apsari[1], Takashi Tanaka[2*]

[1]Gifu University, the United Graduate School of Agricultural Science, Science of Biological Resources, Utilization of Biological Resources, Gifu, Japan. https://orcid.org/0000-0002-1003-8219
[2]Shizuoka University, Faculty of Agriculture, Department of Bioresource Sciences, Shizuoka, Japan. https://orcid.org/0000-0002-7074-7703

***Corresponding author:** tanaka.takashi@shizuoka.ac.jp
Received: February 01, 2022
Accepted: September 25, 2022
Posted online: September 26, 2022

ABSTRACT

An optimum adhesive penetration is needed to provide satisfactory bonding strength at the veneer–veneer interface. The effect of veneer density and glue spreading rate on the phenol formaldehyde adhesive penetration plot profile was determined. An X-ray apparatus was used to visualize the adhesive penetration of the plywood. The heartwood and sapwood veneer of *Cryptomeria japonica* with low, medium, and high veneer densities were made into plywood. The glue spreading rate was applied from 75 g/m^2 to 225 g/m^2 for the heartwood plywood and up to 300 g/m^2 for the sapwood plywood (plus 75 g/m^2 at every level of glue spreading rate). An X-ray apparatus with a low tube voltage successfully visualized the adhesive penetration plot profile. Based on the half-width calculation, the adhesive penetration depth ranged from 0,3 – 0,9 mm. The mean half-width was 0,5 mm. The adhesive concentration increased with increasing glue spreading rate. In contrast, it also showed that using different veneer densities and increasing glue spreading rates does not affect the half-width value as the adhesive penetrates deeper.

Keywords: Adhesive penetration, phenol-formaldehyde, spreading rate, veneer density, X-ray densitometry.

INTRODUCTION

Plywood is a wood product that made from wood veneers glued together with their grains in a perpendicular direction. The important thing of the quality and durability of plywood depends on the adhesive used in manufacturing (Asif 2009). Phenol formaldehyde (PF) is one of the most common moisture-durable adhesives used in plywood. Phenol formaldehyde adhesives are usually used in plywood manufacturing for structural applications in exterior conditions (Kurt 2010, Kurt and Cil 2012). The flow of PF adhesive into the wood cellular structure and infiltration into the cell walls create the wood adhesive interphase (Jakes *et al.* 2015). The pressure applied on the PF adhesive will affect the adhesive penetration (Cognard 2005).

It is important to investigate the adhesive penetration through the adhesive interphase on plywood. Tanaka (2018) developed a geometrical model of wood cells and adhesive penetration at the veneer-veneer interface of plywood. Adhesive penetration is categorized into four scales of penetration, namely, macroscopic penetration, microscopic penetration, nanoscale penetration, and angstrom-scale penetration (Laborie 2002). The depth of adhesive penetration is influenced by adhesive parameters (viscosity), substrate parameters (grain angle; earlywood or latewood), and processing parameters (bonding pressure; open time) (White 1975). Optimum adhesive penetration information is important of the efficiency in using the adhesive (Kurt and Cil 2012).

X-rays can be used to investigate adhesive penetration until microscopic penetration. Since the last century, X-ray has been used for wood inspection (Worschitz 1932, Fisher and Tasker 1940, Tomazello et al 2008) consequently, considering the X-ray apparatus as a

potential tool for quantitative analysis. Based on research conducted by Tanaka *et al.* (2012), the X-ray apparatus can be used to quantitatively measure the moisture content distribution in plywood (Tanaka and Shida 2012). However, limitation of knowledge regarding the quantitative analysis of adhesive penetration in plywood requires further research. In a study by Ferrtikasari *et al.* (2019), it was stated that the qualitative analysis of the X-ray computed tomography image can clearly show the penetration of PF adhesive into lathe check on plywood at a glue spreading rate of 225 g/m^2 and elucidate the relationship between increasing glue spreading rate of plywood and its thermal conductivity (Ferrtikasari *et al*. 2019). Research conducted by Tanaka *et al.* (2015) stated that the PF adhesive in wood can be visualized clearly because the mass attenuation coefficient is different between wood and PF. Thus, the PF adhesive visible to visualize in the wood using X-rays (Tanaka *et al.* 2015).

This study focused to understand PF adhesive penetration size which define as half-width. The effect of increasing glue spreading rate, different wood veneer density, and wood part (heartwood and sapwood part) on the half-width size were investigated. The method to calculate half-width was developed. Other following definition to avoid confusion is term peak-height as PF adhesive concentration.

MATERIALS AND METHODS

Materials

Five-ply sugi (*Cryptomeria japonica*) plywood was made from low-, medium-, and high-density heartwood with density values of 0,281 – 0,309 g/cm^3, 0,319 – 0,343 g/cm^3, and 0,346 – 0.372 g/cm^3, respectively. The medium-density sugi sapwood plywood was made with range of density at 0,320–0,340 g/cm^3. PF adhesive with solid content 48 % was used

77 in this study. Heartwood plywood was made using three glue spreading rates: 75 g, 150 g,
78 and 225 g. Sapwood plywood was made using four glue spreading rates: 75 g, 150 g, 225 g,
79 300 g. Plywood manufacturing was performed by cold-pressing and hot-pressing at 1 MPa
80 for 20 min **(**Ferrtikasari *et al.* 2019) **(**The properties of the X-ray plywood sample are shown
81 in Table 1. Samples for X-ray assessment were cut with dimension 10 mm × 100 mm x
82 plywood thickness for all plywood.

83 **Table 1:** The dimensions and densities of the X-ray plywood samples.

Veneer type	Veneer's density group	Spreading rate (g/m^2)	Dimension (mm)			Weight (g)	Plywood density (g/cm^3)
			R	T	L		
Heartwood	Low	75	10,03	17,31	100,42	6,11	0,351
	Medium		9,39	17,74	98,28	6,54	0,400
	High		10,22	17,89	100,62	7,75	0,421
	Low	150	9,36	16,59	100,00	5,92	0,381
	Medium		10,39	17,13	100,68	7,92	0,442
	High		10,63	17,41	100,34	7,89	0,425
	Low	225	10,33	15,58	100,33	6,92	0,428
	Medium		10,06	16,59	100,80	7,45	0,443
	High		10,23	16,75	100,73	8,36	0,484
Sapwood	Medium	75	9,33	18,08	100,51	5,77	0,340
		150	10,77	17,66	100,48	6,73	0,352
		225	10,13	17,48	100,47	6,61	0,372
		300	10,25	16,90	100,30	6,52	0,375

84

X-ray scanning of plywood

An X-ray apparatus, SR-1010 (Softex Co., Ltd., Ebina, Japan) equipped with a digital X-ray sensor (NX-04H, Softex Co., Ltd.), was used. The sample was scanned on a bondline section with 21.5 kV tube voltage, 3 mA tube current, exposure time of 50 s, and a 416-mm-thick polytetrafluoroethylene (PTFE) filter. A schematic of the X-ray photography set-up is shown in Figure 1.

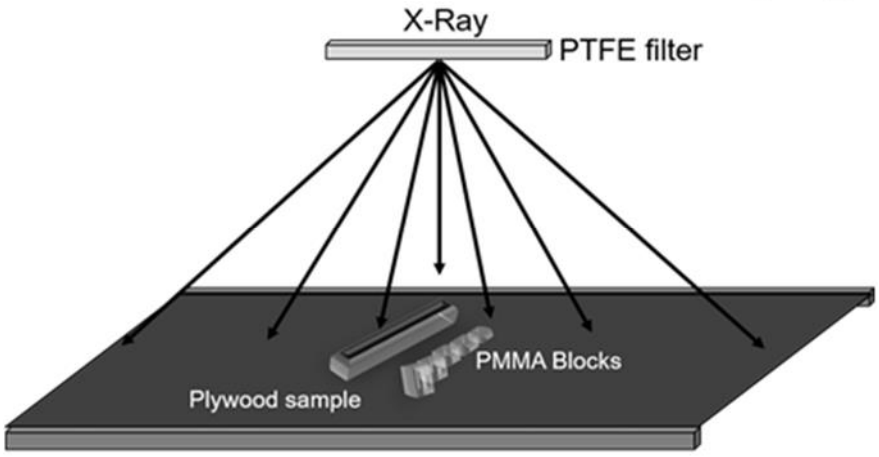

Figure 1: Schematic of the X-ray photography condition.

The X-ray image of the plywood sample was divided into seven lines using ImageJ 1.48v (2014) software to obtain seven plot profiles. The gray value of the poly(methyl methaceylate) (PMMA) block area was used to obtain the equation for the PMMA-equivalent thickness (Figure 2). This equation was used to convert the gray values of the plot profiles. The converted plot profile was calculated using a certain mechanism to obtain the adhesive penetration and adhesive concentration in plywood.

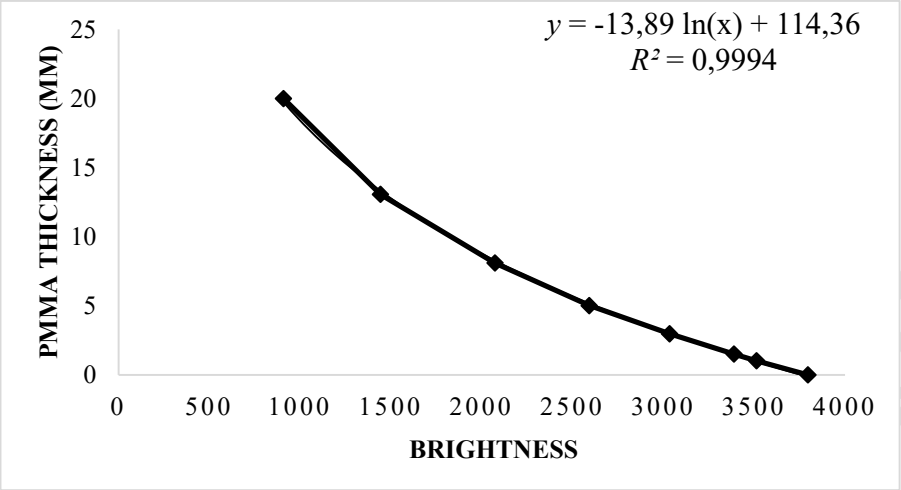

Figure 2: Equation of the PMMA-equivalent thickness.

Statistical analysis

The effects of the glue spreading rate and veneer density on the half-width were analyzed using two-way analysis of variance (ANOVA).

RESULTS AND DISCUSSION

X-ray image of adhesive penetration in sugi plywood

Adhesive penetration was successfully visualized using an X-ray apparatus. Figure 3a clearly shows the plywood X-ray image. The X-ray setting is one of the determinants in the clear and successful visualization of X-ray images. In this study, the low X-ray tube voltage in the X-ray setting was used to visualize the adhesive penetration in heartwood and sapwood plywood with low, medium, and high veneer densities using various levels of glue spreading rates (75 g/m^2, 150 g/m^2, 225 g/m^2 and 300 g/m^2).

The seven-plot profile from seven representative lines on each X-ray image was obtained using ImageJ 1.48. The peak that represented the glue line was pointed out, and the

115 rest were the latewood peaks (Figure 3a). The adhesive that penetrated the lathe check area
116 was estimated to make the glue line peak broader than the glue line, which has no lathe check
117 penetration (Figure 3b). However, the adhesive inside the lathe check has its own peak, which
118 was not part of the general glue line peak.

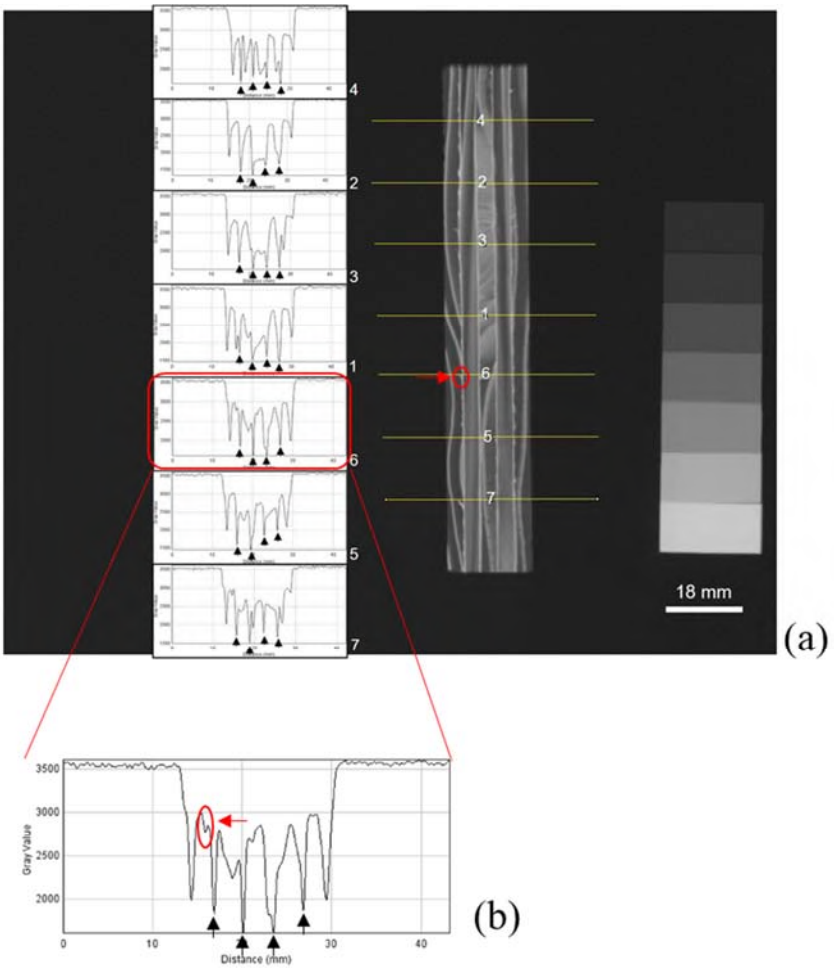

119

120 **Figure 3:** (a) X-ray image of high-density heartwood plywood plot profile with 225 g/m2
121 glue spreading rate with seven adhesive plot profile with the black arrow pointed on the
122 adhesive peak; (b) Lathe check gray value peak pointed by red arrow which separated for
123 adhesive peak.
124

PF adhesive penetration in sugi plywood

The seven-plot profile was converted into a PMMA-equivalent thickness value. This was done in order to understand the penetration of the adhesive in the plywood and the concentration of the adhesive in relation to the glue spreading rate. An example of a successful converted plot profile is shown in Figure 4.

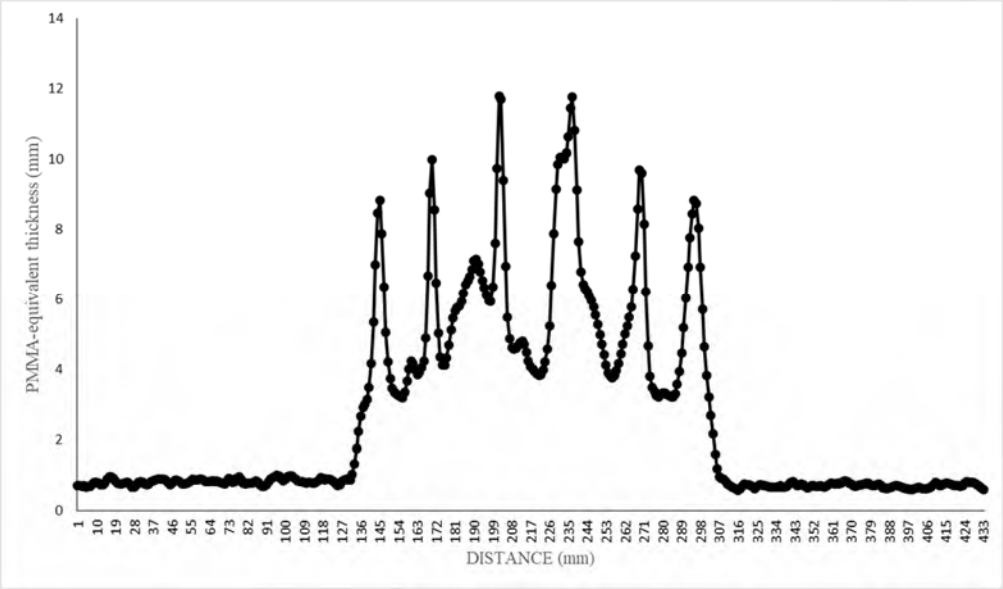

Figure 4: The plot profile of line 6 in high density heartwood plywood with 225 g/cm^2 glue spreading rate that successfully converted using PMMA equation from PMMA calibration curved.

After converting the plot profile, the mechanism for calculating the penetration depth of the glue was developed in this study and is shown in Figure 5.

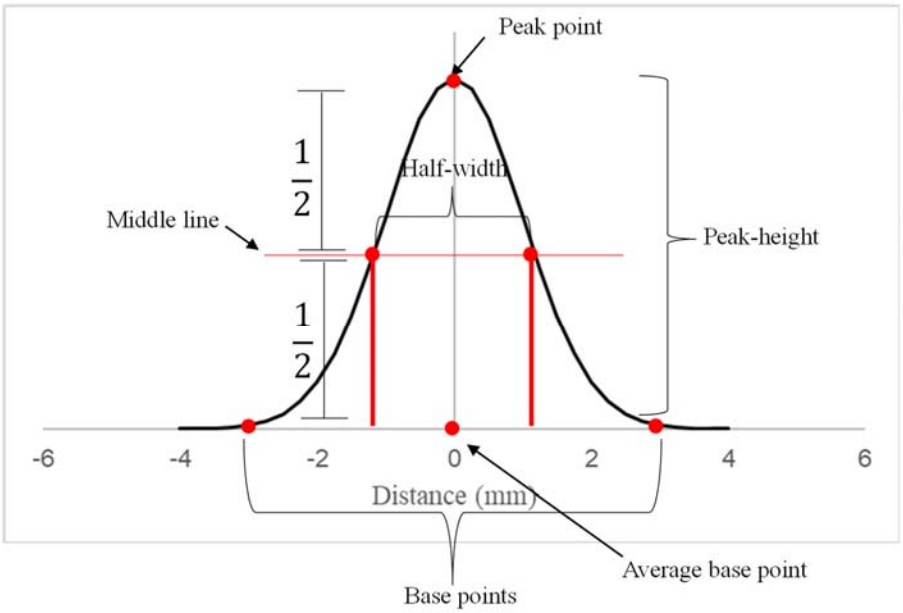

Figure 5: The mechanism of calculated the peak height and half-width.

The base point of the peak should be determined based on the horizontal inequality position of the base point. After the peak height was obtained, the height of the graph was divided by two, which was the way to obtain the middle line of the graph. Then, the length of the middle line of the graph, which is defined as the half-width occurred. The half-width of the peak was considered as the adhesive penetration depth. The peak height was considered as the adhesive concentration. The half-width and peak-height were obtained from the calculation of the glue line peak (Figure 6). The half-width (adhesive penetration) value obtained from various glue spreading rate and veneer density was investigated to see the relations between them (Figure 7).

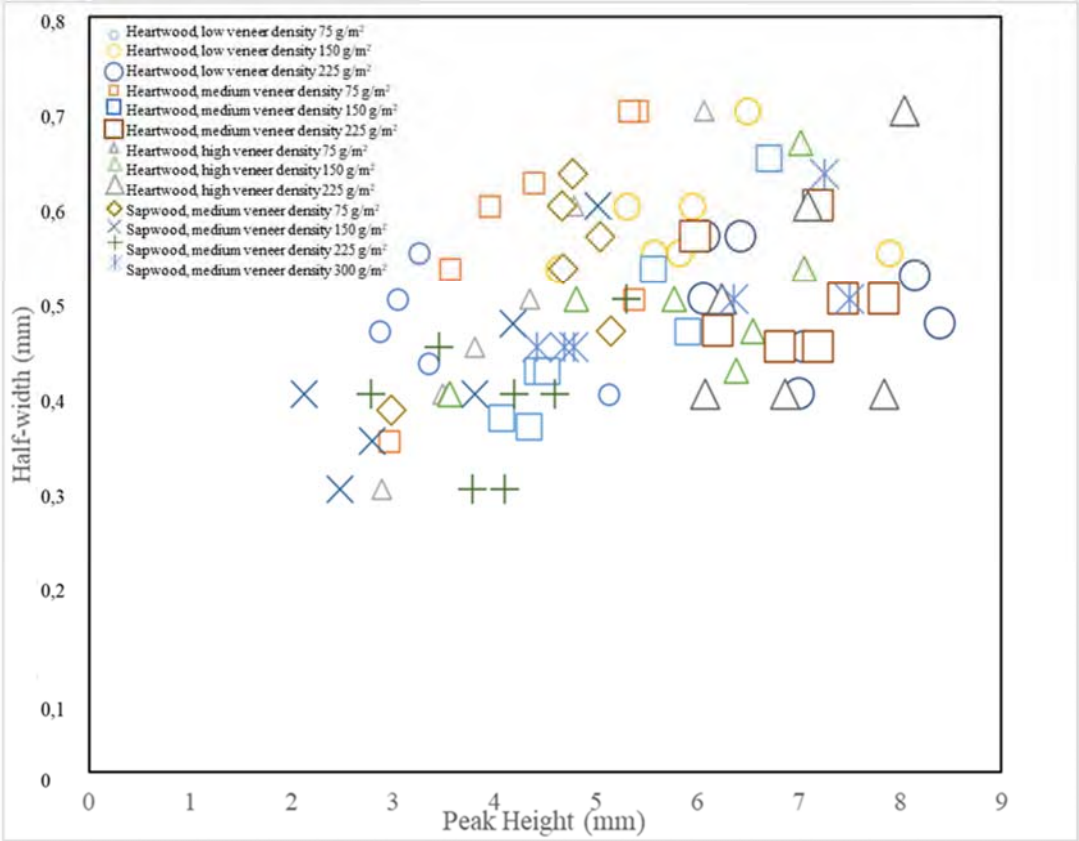

Figure 6: Seven points of peak height and half-width of low, medium, and high veneer density heartwood plywood with 75, 150, 225 g/m^2 glue spreading rate; and medium veneer density sapwood plywood with 75, 150, 225, and 300 g/m^2 glue spreading rate.

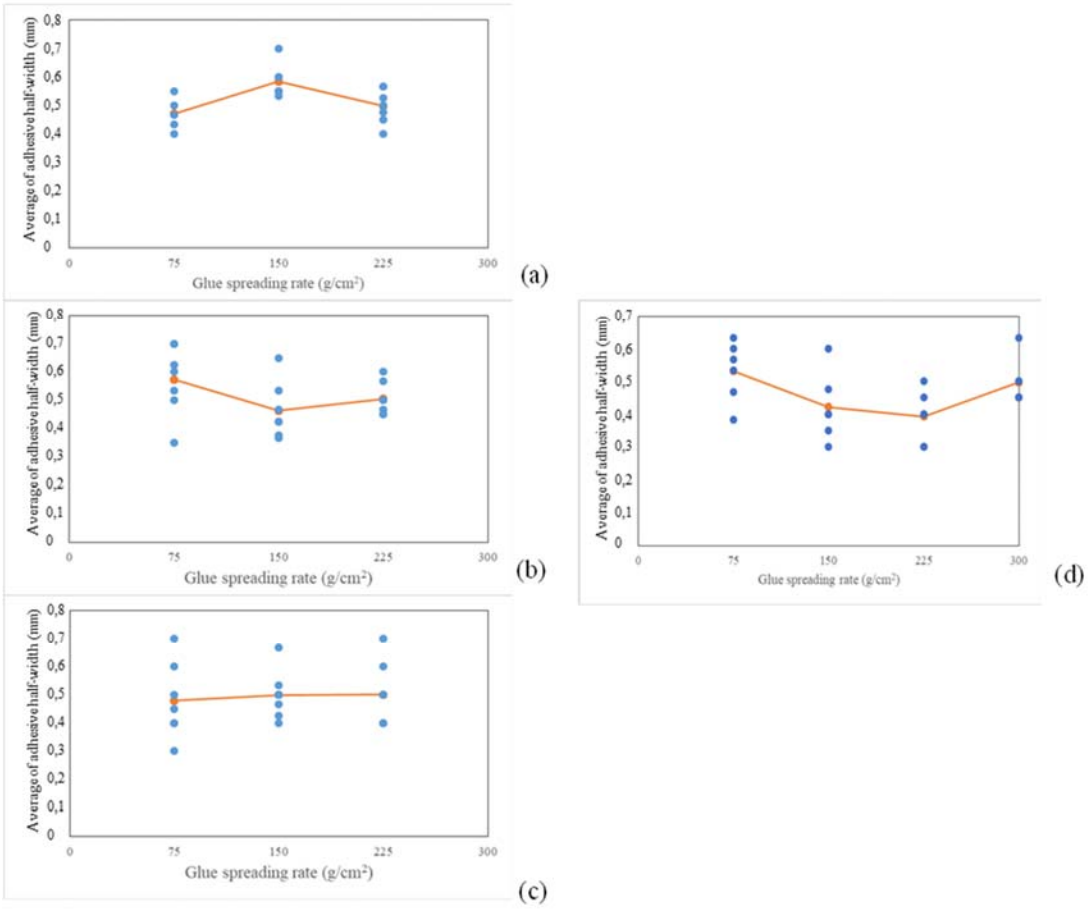

153

154 **Figure 7:** PF adhesive half-width of (a) low density heartwood plywood, (b) medium density
155 heartwood plywood, (c) high density heartwood plywood, and (d) medium density sapwood
156 plywood.
157

158 The half-width was within the range of 0,3 mm to 0,9 mm and was approximately 0,5
159 mm on average, regardless of the glue spreading rate or veneer density. This finding is similar
160 to that reported by Modzel *et al.* in 2011 that the penetration depth of the adhesive in the oak,
161 Douglas-fir, and poplar were 400 μm, 100 μm, and 400 μm, respectively (Modzel *et al.* 2011).
162 These results support the idea that glue penetration into the veneer in plywood manufacturing

is constant, regardless of the glue spreading rate, veneer density, or the wood species of the veneer. The smallest half-width value (= 0,3 mm) occurred near the boundary between earlywood and latewood (Figure. 8), suggesting that the existence of latewood in the veneer might limit the adhesive penetration. This limitation may lead to the consistency of the average half-width value without regard to the glue spreading rate or veneer density.

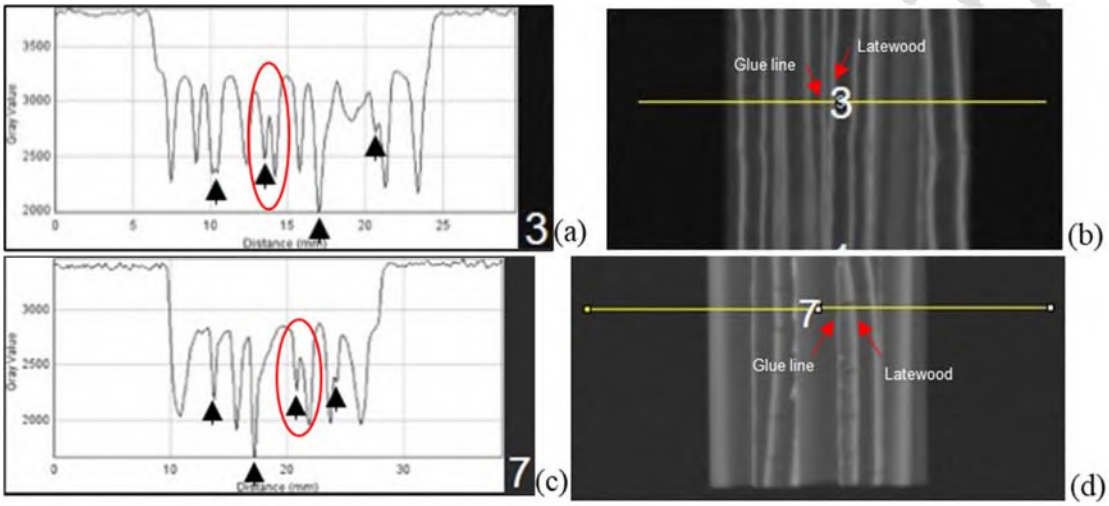

Figure 8: The X-ray image and its plot profile which indicates the smallest half-width value (0.3 mm). (a) A plot profile of medium veneer density of sapwood plywood with 150 g/m^2 glue spreading rate and (b) its X-ray image, and (c) a plot profile of high veneer density of heartwood plywood with 75 g/m^2 glue spreading rate and (d) its X-ray image.

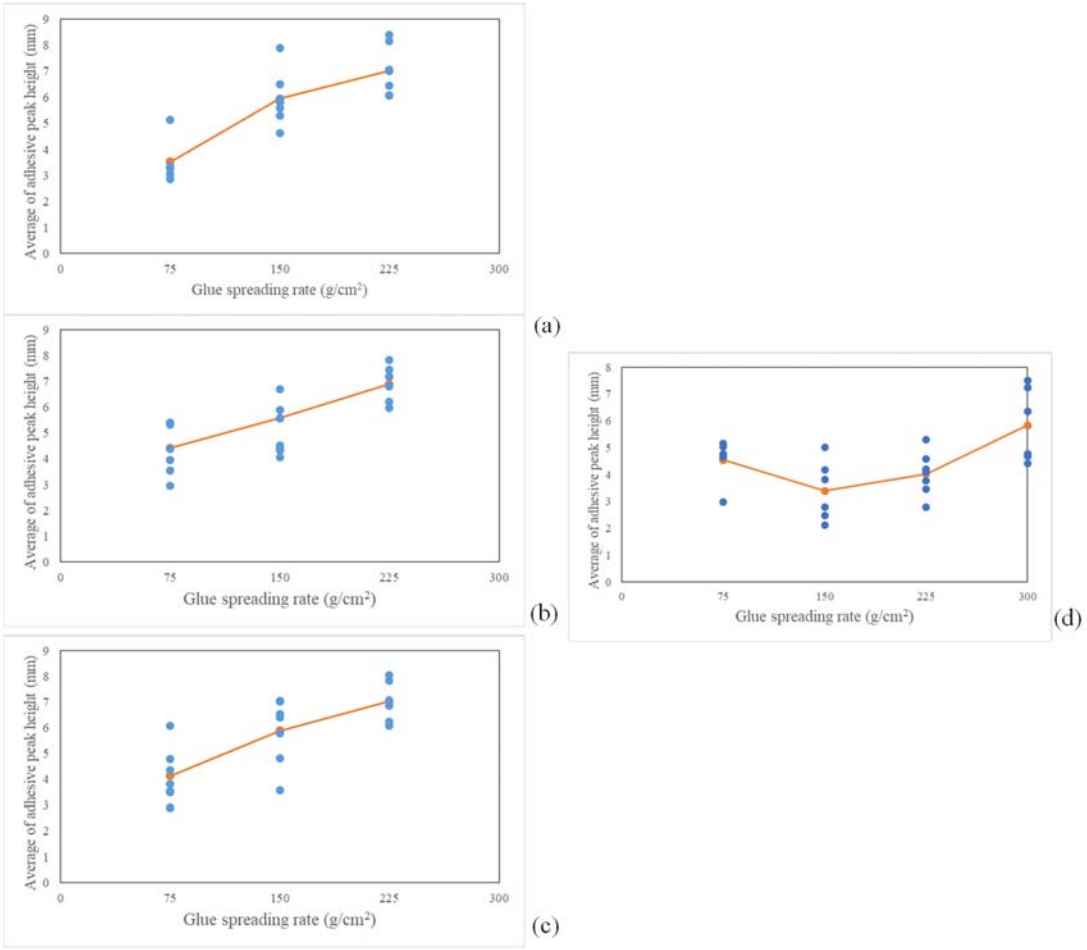

Figure 9: PF adhesive peak height of (a) low density heartwood plywood, (b) medium density heartwood plywood, (c) high density heartwood plywood, and (d) medium density sapwood plywood.

The adhesive concentration (peak height) increased along with increasing the glue spreading rate. The peak height of the heartwood plywood with low, medium, and high veneer densities showed the same trend (Figures 9a, 9b and 9c). The peak height increased with increasing glue spreading rate. In addition, regarding the sapwood-veneer plywood, the maximum peak height was obtained at the maximum spreading rate of 300 g/m^2 (Figure 9d).

183 These results indicate that the concentration of the adhesive at the bondline is increased by
184 increasing adhesive spreading rate.

185 The statistical analysis using two-way ANOVA method did not reveal any significant
186 effect of glue spreading rate, veneer density, or their interactions on the half-width value
187 (Table 2).

188 **Table 2:** Results of the two-way ANOVA of veneer density and glue spreading rate in
189 relation with PF adhesive penetration (half-width) on Sugi heartwood plywood.

Variation factor	Sum of squares	Degree of freedom	Mean of Squares	F value			F critical (5%)
Veneer Density	0,009294	2	0,004647136	0,511127732	<		3,18
Spreading rate	0,002184	2	0,001091854	0,120090442	<		3,18
Interaction	0,086737	4	0,021684153	2,384989672	<		2,56
Residue	0,463688	51	0,009091927				
Total	0,561903	59					

190

191 ## CONCLUSIONS

192 We successfully evaluated the concentration profile of sugi plywood with a low X-
193 ray tube voltage. The PF adhesive penetration in the sugi plywood had values of 0,3–0,9 mm,
194 with an average of 0,5 mm. In this experiment, using sugi plywood, it was shown that the
195 existence of latewood might limit the PF adhesive penetration. On the other hand, the PF
196 adhesive concentration in the glue line increases with increasing veneer density and glue
197 spreading rate. Findings from this study would be useful in the analysis of a plywood's
198 quality and durability.

ACKNOWLEDGEMENTS

This study was supported by JSPS KAKENHI grant numbers 17H05032 and 20K06163. We thank J-Chemical Co., Ltd. for supplying the phenol formaldehyde adhesive, and NODA Corporation for supplying the sugi veneer. We are grateful to Ms. Nindya Ferrtikasari for preparing the plywood samples. We thank Ms. Aoi Oishi for statistical analysis.

REFERENCES

Asif M. 2009. Sustainability of timber, wood and bamboo in construction. Chapter 2: 31-54. In: *Sustainability of construction materials*. Khatib JM (ed.), Woodhead Publishing, Sawston, United Kingdom. https://doi.org/10.1533/9781845695842.31

Cognard P. 2005. Technical characteristics and testing methods of adhesives and sealants. Chapter 2: 21-99. In: *Handbook adhesive and sealants*. Cognard P (ed.), Elsevier, Oxford, United Kingdom. https://doi.org/10.1016/S1874-5695(02)80003-3

Ferrtikasari, N.; Tanaka, T.; Yamada, M. 2019. Relationship between thermal conductivity and adhesive distribution of phenol-formaldehyde visualized with x-ray computed tomography on sugi (*Cryptomeria japonica* D.Don) heartwood plywood. In: *IOP Conference Series: Materials Science and Engineering*, Volume 593, The 14th Pacific Rim Bio-Based Composites Symposium 29–31 October 2018, South Sulawesi Province, Indonesia. http://dx.doi.org/10.1088/1757-899X/593/1/012003

Fisher, R.C.; Tasker, H.S. 1940. The detection of wood boring insects by means of X-rays. *Annals Applied Biology* 27(1):92-100

Jakes, J.E.; Hunt, C.G.; Yelle, D.J.; Lorenz, L.F., Hirth, K.; Gleber, S-C., Vogt, S.; Grigsby, W.; Frihart, C.R. 2015. Synchrotron-based X-ray fluorescence microscopy in conjunction with nanoindentation to study molecular-scale interactions of phenol-formaldehyde in wood cell walls. *ACS A ppl Ma ter Interfaces* 7: 6584-6589. https://doi.org/10.1021/am5087598

Kurt, R. 2010. Possibilities of using poplar clones and boron compounds to manufacture fire resistant laminated veneer lumber. In: Project No: 106O556 progress report, Turkish Scientific Research Council, Kavaklıdere / Ankara, Türkiye.

Kurt, R.; Cil, M. 2012. Effect of press pressures on glue line thickness and properties of laminated veneer lumber glued with phenol formaldehyde adhesive. *BioResources* 7(4): 5346-5354. https://ojs.cnr.ncsu.edu/index.php /BioRes/article/view/3200

Laborie, M-P.G. 2002. Investigation of the Wood/Phenol-Formaldehyde Adhesive Interphase Morphology. PhD Dissertation, Virginia Polytechnic Institute and State University, Virginia, The United State of America.

Modzel, G.; Kamke, F.A.; De Carlo, F. 2011. Comparative analysis of a wood: Adhesive bondline. *Wood Sci Technol* 45: 147–158. https://doi.org/10.1007/s00226-010-0304-z

Open-source Java image processing program 2014. ImageJ 1.48v. Retrieved from http://imagej.net/

Scheikl, M. 2002. Properties of the glue line – Microstructure of the glue line. In: *Wood Adhesion and Glued Products: Glued Wood Products State of the Art Report.* Johansson, C.J.; Pizzi, T.; Van Leemput, M. (eds.), COST Action E13. 109-111p. http://users.teilar.gr/~mantanis/E13-Wood-Adhesion.pdf.

Tanaka, T. 2018. Simple geometrical model of thermal conductivity and bound-water diffusion coefficient in resin-rich regions of softwood plywood. *Wood Sci Technol* 52: 331–342. https://doi.org/10.1007/s00226-018-0985-2

Tanaka, T.; Adachi, K.; Yamada, M. 2015. X-ray mass attenuation coefficient for some common wood adheives in the tube voltage range from 15 kV to 100 kV. *Mokuzai Gakkaishi* 61(5): 308-315. https://doi.org/10.2488/jwrs.61.308

Tanaka, T.; Shida, S. 2012. Changes of Through-thickness Moisture Distribution in Wood and Wood-based Materials in Adsorption Phase III. Nondestructive measurement of moisture content distribution in plywood and sheathing insulation fiberboards. *Mokuzai Gakkaishi* 58(5): 271-278. https://doi.org/10.2488/jwrs.58.271

Tomazello, M.; Brazolin, S.; Chagas, M.P.; Oliveira, J.T.S.; Ballarin, A.W.; Benjamin, C.A. 2008 Application of x-ray technique in nondestructive evaluation of eucalypt wood. *Maderas-Cienc Tecnol* 10: 139–149. https://doi.org/10.4067/S0718-221X2008000200006

White, M.S. 1975. Influence of Resin Penetration on the Fracture Toughness of Bonded Wood. PhD Dissertation, Virginia Polytechnic Institute and State University, Virginia, The United State of America.

Worschitz, F. 1932. L'utilization des rayos. In: Congrès IUFRO, X en vue de l'etude de la qualité du bois Paris. France, pp 459–489. (In French).